

General Disclaimer

One or more of the Following Statements may affect this Document

- This document has been reproduced from the best copy furnished by the organizational source. It is being released in the interest of making available as much information as possible.
- This document may contain data, which exceeds the sheet parameters. It was furnished in this condition by the organizational source and is the best copy available.
- This document may contain tone-on-tone or color graphs, charts and/or pictures, which have been reproduced in black and white.
- This document is paginated as submitted by the original source.
- Portions of this document are not fully legible due to the historical nature of some of the material. However, it is the best reproduction available from the original submission.

NATIONAL AERONAUTICS AND SPACE ADMINISTRATION

Technical Memorandum 33-618

*Processing of Thermionic Power on an
Electrically Propelled Spacecraft*

T. W. Macie

(NASA-CR-135941) PROCESSING OF THERMIONIC POWER ON AN ELECTRICALLY PROPELLED SPACECRAFT (Jet Propulsion Lab.) 67 p
HC \$5.50 CSCL 21C G3/28 N74-10727
Unclas 21066

JET PROPULSION LABORATORY
CALIFORNIA INSTITUTE OF TECHNOLOGY
PASADENA, CALIFORNIA

November 1, 1973

NATIONAL AERONAUTICS AND SPACE ADMINISTRATION

Technical Memorandum 33-618

*Processing of Thermionic Power on an
Electrically Propelled Spacecraft*

T. W. Macie

JET PROPULSION LABORATORY
CALIFORNIA INSTITUTE OF TECHNOLOGY
PASADENA, CALIFORNIA

November 1, 1973

PRECEDING PAGE BLANK NOT FILMED

PREFACE

The work described in this report was performed by the Propulsion Division of the Jet Propulsion Laboratory.

7

ACKNOWLEDGEMENT

The author wishes to express his gratitude to all those who offered help and counsel, in particular to D. Ferg, T. Hsieh, J. Mondt, A. Nakashima, and J. Stearns of Jet Propulsion Laboratory, and F. Kelley, Jr., and C. Sawyer of General Electric.

CONTENTS

I.	Scope of the Study	1
A.	Introduction	1
B.	Requirements	1
C.	Design Variables	2
II.	Configuration	3
A.	General	3
B.	Power Conditioners	4
C.	Power Inverters	5
D.	Reliability	6
III.	Parametric Study Results	8
A.	Optimum Frequency	8
B.	Electrical Efficiencies	8
C.	Parameter Sensitivities	8
1.	Inverter Mass	8
2.	Power Processor Mass	9
3.	TFE-Source Voltage	9
4.	Power Transistors	9
5.	Magnetic Materials	10
IV.	Conclusions and Recommendations	10
A.	Conclusions	10
B.	Recommendations	10

CONTENTS (contd)

Appendix A.	Power Conversion	28
Appendix B.	Radiators	39
Appendix C.	Inverter Design	43
References	56
Symbols	57

TABLES

1.	Environmental conditions	11
2.	TFE unit sources, characteristics	12
3.	Number (N) of TFE-source/inverter modules	12
4.	NEP power conditioner, power, efficiency, and losses	13
5.	Efficiencies for different sources	14
6.	Assumed power transistor characteristics	14
A-1.	Skin effect penetration depth (p) and AWG-wire size for different frequencies	31
B-1.	Radiator specific mass	42
C-1.	ATH core sizes and design parameters	52
C-2.	Wire data	53
C-3.	Power distribution mass, G7	54
C-4.	Power conditioners (27) mass, G8	54

FIGURES

1.	Nuclear electric propulsion power processing configuration	15
2.	Power distribution from ac bus to loads	16
3.	Auxiliary thruster power distribution	17
4.	Mass of radiators vs environmental conditions	18

CONTENTS (contd)

FIGURES (contd)

5.	Regulated power inverter, 3 phase	19
6.	Power subsystem, N modules	20
7.	S5 specific mass, 8-V source, inverter plus radiator plus source mass penalty	21
8.	S5 specific mass, 23-V source, inverter plus radiator plus source mass penalty	22
9.	S5 specific mass, 40-V source, inverter plus radiator plus source mass penalty	23
10.	Mass of inverters and distribution cables for various source voltages	24
11.	Mass and specific mass power processor for different source voltages	25
12.	Variation of mass of power processor with 8-V source for various transistor types	26
13.	Variation of efficiency and source mass penalty of power processor with 8-V source for various transistor types	27
A-1.	Input and output voltages, power inverter module	32
A-2.	Transistor losses for three types of transistors, 8-V power inverter	33
A-3.	Transistor losses for two types of transistors, 23-V power inverter module	34
A-4.	Transistor losses for two types of transistors, 40-V power inverter module	35
A-5.	Core dimensions	36
A-6.	Core loss curves, 2-mil Permalloy	37
A-7.	Power inverter output voltage control	38
C-1.	Three-phase E-core cross section and the middle length of a turn (L_2)	55

ABSTRACT

A study was conducted at the Jet Propulsion Laboratory to define the power processing equipment required between a thermionic reactor and an array of mercury-ion thrusters for a nuclear electric propulsion system. A new concept of electric power processing that can satisfy all the guidelines and requirements imposed by the thermionic-fuel-element power source and all the user loads has been proposed and evaluated.

Observations and recommendations that resulted from this study were: (1) the preferred thermionic-fuel-element source voltages are 23 V or higher; (2) transistor characteristics exert a strong effect on power processor mass; (3) the power processor mass could be considerably reduced should the magnetic materials that exhibit low losses at high frequencies, that have a high Curie point, and that can operate at 15 to 20 kG become available; (4) electrical component packaging on the radiator could reduce the area that is sensitive to meteoroid penetration, thereby reducing the meteoroid shielding mass requirement; (5) an experimental model of the power processor design should be built and tested to verify the efficiencies, masses, and all the automatic operational aspects of the design.

I. SCOPE OF THE STUDY

A. Introduction

A study was conducted at JPL to define the power processing equipment required to link a thermionic reactor and an array of mercury-ion thrusters of a nuclear electric propulsion (NEP) system. The "Flashlight" thermionic reactor, under development by Gulf General Atomic for the Atomic Energy Commission, was used as a basis for this study. Each thermionic power source consists of a certain number of thermionic fuel elements (TFEs), in a series-parallel configuration, that supply the electrical power to the power processing equipment. Each TFE generates approximately 1 kW at 4 Vdc.

The study had two basic objectives: first, to identify a power processing equipment configuration that satisfies the general requirements of the NEP spacecraft and, second, to identify and parametrically study the design that offers the minimum subsystem mass. The parametric study was accomplished by means of a computer programmed to define the impact of environmental conditions on the subsystem mass. It included a calculation of the mass of components and structure over a range of inverter frequencies, a determination of electrical efficiencies of the power processor with different input voltages, and identification of critical problem areas and major mass and performance penalties.

B. Requirements

The general requirements were defined as follows:

- (1) The solar electric power conditioning technology will be used, wherever feasible, to minimize development cost.
- (2) Load sharing by all TFE sources for all electrical power loads must be ensured.
- (3) The power processing equipment must be capable of operating at 50% of input voltage. This is required to accommodate partial power operation, partial source failures, and position-dependent variations in source power voltage levels.

- (4) The conceptual design of the power processor must be compatible with the thermionic reactor control scheme, which calls for maintaining a constant user load voltage with varying power demands and varying input voltages.
- (5) The TFE sources must be isolated from thruster arcing.
- (6) Single-point failures shall be eliminated. Unavoidable single-point failure modes shall be analyzed and steps taken to assure an acceptable reliability.
- (7) A 20% redundancy in all TFE-unit sources, inverter modules, power conditioners, and thrusters will be provided. This requirement may be revised following reliability studies to determine the adequacy and/or necessity of that redundancy.

A block diagram of the selected NEP baseline power processing configuration is shown in Fig. 1. The power subsystem is modular, and consists of a number of thermionic power sources electrically connected to the same number of power inverters, which step up a low-output dc voltage of the source to a high ac voltage of the bus. The high-voltage ac distribution bus feeds the electrical power to the various users. Power could also be distributed in the form of dc; this report, however, is limited to a study of the ac concept only. Each user employs a power conditioner (PC) to condition the ac power to meet the needs.

C. Design Variables

To gain an insight into how the overall power subsystem's mass is affected by the environmental conditions that prevail, by the type of TFE source that is employed, and by the critical electrical parameters of concern, a series of designs was performed.

The radiator mass was calculated for three environmental conditions: first, radiator surface temperature; second, space temperature; third, inclusion or exclusion of meteoroid protection. Table 1 lists eight variants that were individually studied. Because the spacecraft designer is interested in knowing what penalty in mass has to be paid for a corresponding gain in reliability, two radiator surface temperatures were considered: 50°C and 100°C, the latter corresponding to the semiconductor junction temperatures approximately 25°C higher than the former. Effective sink

temperatures of 150 K and 250 K were used for sizing the radiators (Appendix B); these are mission-averaged sink temperatures that might be encountered on a typical geocentric and outer-planet space mission (Ref. 1). The inclusion or exclusion of the meteoroid protection was mission dependent; for missions where spacecraft had to penetrate the asteroid belt, such protection would most likely be required. For further details, see Appendix B.

The TFE source characteristics also impact upon the mass of the power inverter. Three different source voltages were selected for study (Table 2): 8 V, 23 V, and 40 V. To identify the design that offers the minimum power subsystem mass, the carrier frequency at which the power inverters operate was varied from 1 to 15 kHz. The density of the magnetic flux in the transformer Permalloy-cores was not allowed to exceed 6.5 kG, whereas the current density in the transformer coils was kept below 2500 A/in.²; any design for which either of these two conditions was not met was rejected and another design using a larger size core was performed.

II. CONFIGURATION

A. General

For the purpose of this study, the power subsystem consisted of the thermionic power sources and power inverters, whereas the thrust subsystem consisted of power conditioners and ion thrusters. The power inverters and power conditioners combined are referred to as the power processor. The following power requirements were assumed:

- (1) PC input power, 120 kW.
- (2) All other power and spacecraft power, 8.0 kW.

The total power at the high-voltage ac bus, therefore, amounted to 128 kW (Fig. 2).

A modular approach was used with a number of power sources operating in parallel. Table 2 presents a description of the power sources considered. The total number (N) of TFE-source/inverter modules required for 120 kW for different types of thermionic power sources is listed in Table 3.

The power inverters and the thrust subsystem power conditioners were linked by a three-phase, ac distribution bus. The voltage of this bus was maintained constant and independent of the configuration of the source. The power required for the spacecraft and the housekeeping loads in the power subsystem was also supplied from this ac distribution bus. Losses in the power inverters and distribution were calculated to be approximately 5 to 6% (see Subsection III-B, below).

B. Power Conditioners

The power requirements of a single mercury-ion thruster operating at $I_s = 4000$ s for nuclear-electric propulsion are presented in Table 4. This table has been derived from the requirements of the solar electric propulsion technology (Refs. 2 and 3) and represents the best estimate presently available. On this basis, the PC efficiency was derived as:

$$\eta = \frac{5200}{5200 + 275.4} = 95\%$$

The thruster beam power, which generates the thrust, amounted to 4 kW while the thruster auxiliary power (10 loads) equaled approximately 1.2 kW. Initially, 22 thruster-PC sets were used for the propulsion with five sets retained as spares.

The total power was distributed as shown in Fig. 2. It should be noted that the beam power rectifier was connected directly to the three-phase ac bus and no additional transformation was required. Thyristor bridges were used to rectify and regulate the individual outputs. The rectification stages were followed by appropriate filter stages.

The auxiliary power for the thruster was transformed to a 50-V, three-phase, ac level and then distributed as shown in Fig. 3. The 50-V ac power was selected to eliminate the need for any additional transformation for the arc discharge power, since the arc power was by far the largest auxiliary load. Figure 3 represents the auxiliary power concept that was developed for solar electric propulsion (Refs. 2 and 3).

The mass of all the component parts of one PC, excluding the radiators, has been estimated to be 10 kg. This estimate was based on data available

from the solar electric technology program (Ref. 3). The mass of PC radiators varied, depending on environmental conditions imposed (Table 1); the results of the parametric study of radiator mass are shown in Fig. 4. For further detail, see Appendix B.

C. Power Inverters

Two three-phase inverters, a master and a slave, were connected to each of the TFE sources (Fig. 5) to provide a regulated, three-phase, ac output. The master/slave pair is referred to as a "power inverter module" or simply, an "inverter".

The detailed description of the power inverter module including the principles of regulating for a constant output voltage are presented in Appendix A. The total power of the ac distribution bus (Fig. 1) can be obtained by connecting the outputs of individual power inverters either in parallel or in series. A series connection scheme was chosen for the NEP system (Fig. 6) because it provides a convenient method for obtaining high voltages, as required for ion thrusters, and it inherently satisfied the requirement for load sharing among all the TFEs.

Design of the power inverter consisted of selecting the type of the transistors, determining the size of radiators, and designing the output transformers.

Selection of the type of power transistors was performed according to procedures of Appendix A; transistor losses were calculated by hand and are shown in Figs. A-2, A-3, and A-4; mass of the power transistors and the drivers, complete with the mounting hardware, was estimated to be 150 g.

The radiators were designed according to procedures described in Appendix B. Table B-1 lists the radiator specific mass, in kg/kW loss, for all eight environmental cases (Table 1).

The output transformers were designed by computer according to procedures described in Appendix C.

For the 8-V TFE source, for instance, the procedure for obtaining the data shown in Fig. 7 was as follows:

- (1) At a specified operating frequency, the transistor and its losses are selected from Fig. A-2. Maximum current density in

copper and maximum magnetic flux density in iron are specified. With these inputs, the computer designs the transformer (see Appendix C, Eqs. C-1 to C-36), and for each environmental case, sizes the radiators (Eq. C-38) and determines the specific mass (S4) of the power inverter (Eq. C-42).

- (2) Since inverter power losses exact a mass penalty from the TFE source (i. e., each watt of loss adds to the mass of the source), this mass penalty must be added to the actual specific mass of the inverter. The penalty imposed was assumed to be 20 kg/kWe for the 8-V source, and 15 kg/kWe for the 23-V and 40-V sources. The true specific mass of the inverter with source losses (S5) is then determined (Eq. C-43).
- (3) Copper current density and magnetic flux density are varied, and the computer selects the appropriate transformer core and designs the power inverter. As a result, the lowest S5 design is identified at the selected operating frequency.
- (4) Next, frequency is specified, and the design optimization repeated. This is continued over the range of frequencies of interest.

The same procedure was used for optimizing the designs for 23-V (Fig. 8) and 40-V (Fig. 9) TFE sources.

D. Reliability

The reliability analysis of the power processing hardware is a formidable task in its own. Therefore, no attempt to develop the appropriate reliability model or define the theoretical reliability of the configuration was made. However, an attempt was made to identify the critical design problem areas and to define a power processor capable of surviving any single module failure.

To permit operation with failed modules, a redundancy amounting to 20% of excess capacity was provided. Initially, when no components had failed, all the TFE power sources operated at 80% of full power; twenty-two thrusters were operating, five thrusters were shut off.

The effect of power source or power load failures on the power processors was examined to ensure that the power processor design was compatible.

In the case of an open- or short-circuit failure of one TFE source, the power flow through the corresponding power inverter module is zero. To prevent energy feedback from the high-voltage bus into the associated power inverter, the output transformer of this module must be kept saturated. To keep the transformer saturated, all the power transistors of the corresponding power inverter must be turned fully on. To compensate for the loss of voltage on the high-voltage bus, the output voltage of each series-connected power inverter is automatically increased. The increased voltage is obtained by means of the electronic control of the master/slave combination. Should the power inverter fail while the TFE source is operable, it is desirable that the TFE source experiences a short-circuited load. This prevents excessive temperature increase in the TFE. As in the previous case, this can be accomplished by turning on all the power transistors of the disabled power inverter. As before, the high-voltage bus voltage is maintained constant by increasing the output voltage of each of the operating inverters.

Another potential failure mode within the inverter module is a failure in the output transformer. The most critical failure mode would be an open circuit in the transformer secondary winding. The secondary windings of all the transformers are series connected to produce the high voltage, so an open circuit in any transformer secondary could mean loss of all power. To avoid such failure, each transformer secondary is wound with four or five wires in parallel. The individual wires from each transformer may, if necessary, be connected in series through separate connectors or soldering points. Failure of one wire will not disrupt the module's operation and will not cause overheating because the remaining three or four wires are sized for carrying a 20 to 25% higher current.

The thrust subsystem configuration selected for NEP has thrusters and power conditioners permanently coupled (Fig. 2). A failure of either the power conditioner or the thrusters disables the entire set. In the case

of the failure of a thruster or power conditioner, the power to that set is automatically turned off and a spare set started.

Random arcing between the grids of the thruster necessitates the interruption of the beam power. Beam power interruption and clearing the dc arc is performed by the power conditioner electronics that turn off the thyristor bridge rectifier (Fig. 2). The self-commutation of the thyristor bridge is possible because of the ac characteristics of the high-voltage bus.

All auxiliary thruster power is derived from a 50-V ac bus (Fig. 3). For reliability reasons, two step-down transformers connected in parallel have been used; each is capable of carrying the full load. Fuses will automatically disconnect a failed transformer.

III. PARAMETRIC STUDY RESULTS

A. Optimum Frequency

The specific mass optimization study, described above, has established designs at which the S5 specific mass became minimum. The S5 vs frequency plots are shown in Figs. 7 to 9. Based on these curves, 2 kHz was selected for the 8-V system and 7 kHz for the 23-V and 40-V systems. The three selected designs were then parametrically studied. The following presents the results of this analysis.

B. Electrical Efficiencies

The electrical efficiencies of the power processor for the three source voltage levels investigated are shown in Table 5. The efficiency represents the best power subsystem design. Lower efficiencies penalized the mass of TFE-sources and radiators, higher efficiencies impacted unfavorably on the mass of the power inverters.

C. Parameter Sensitivities

1. Inverter Mass. The mass of all the inverters plus the mass of the electrical power distribution cables for different source voltages and environmental conditions (cases 1 through 8 of Table 1) are shown in Fig. 10. It is evident that the 8-V system is the heaviest, the 40-V system lightest; in case 8 the difference amounts to 275 kg. At each level of input voltage,

the bandwidth between cases 6 and 8 amount to approximately 200 kg, between cases 1 and 4 to 100 kg.

2. Power Processor Mass. For the type of TFE source used, the specific mass of the power processor (Fig. 11) varies between 5.3 and 10.5 kg/kW for the 8-V system, 3.8 and 9.3 kg/kW for the 23-V system, and 3.5 and 8.5 kg/kW for the 40-V system.

The meteoroid shielding (cases 5 to 8 of Table 1) contributes greatly to the mass penalty. For example, the 23-V system with no meteoroid protection exhibits a specific mass variation for different radiator/sink temperature combinations of 3.5 to 5.2 kg/kW. With meteoroid protection, the 23-V system specific mass varies from 5.5 to 9.3 kg/kW. This is a 1.7 to 3.8 kg/kW specific mass penalty for meteoroid armor.

Comparison of cases 1 to 3 with 2 to 4 (no meteoroid protection) shows the mass penalty incurred by reducing the radiator temperature from 100°C to 50°C. It can be seen that for the 23-V case the specific mass increases from 3.8 kg/kW to 4.5 kg/kW (150-K effective sink temperature in deep space), or from 4 kg/kW to 5.2 kg/kW (250-K effective sink temperature in near-earth space). Similarly, for cases 5 and 7, and 6 and 8 (with meteoroid protection), the specific mass changes from 5.2 kg/kW to 7.3 kg/kW (150-K sink temperature), or from 6 to 9.3 kg/kW (250-K sink temperature).

The effects of the space sink temperature can be determined by comparing cases 1 to 2, 3 to 4, 5 to 6, and 7 to 8. As expected, the mass is much more sensitive to space sink temperature at lower radiator surface temperature.

3. TFE-Source Voltage. The mass of the power processor, as shown in Fig. 11, is very dependent on the source voltage. In cases 1 to 4 of Table 1, where no meteoroid protection is required, the penalty increases rapidly as the TFE-source voltage is reduced below the 23-V level. In cases where meteoroid shielding is provided, the penalty increases with low voltages are less pronounced, however the power processor mass is still very dependent on the input voltage level.

4. Power Transistors. The optimum efficiency and minimum mass of the power processor is significantly affected by the characteristics

of the power transistors used in the power inverter. The assumed power transistor saturated forward voltages ($E_{CE\ sat}$) and switching times (T_{SW}) are listed in Table 6. The related details can be found in Appendix A.

The way in which the transistor characteristics affect the power processor mass (G9), when operating from an 8-V source, is shown in Fig. 12. Figure 13 shows how the efficiency and the source mass penalty (S6) vary with the transistor characteristics for the 8-V source configuration. It can be seen that the transistor characteristics greatly affect the mass and efficiency of the power processor. Also the optimum operating frequency is influenced by transistor characteristics. For each type of transistor, a different optimal carrier frequency was obtained (Fig. 12). As the specific mass of the processor increases from case 1 to case 8 of Table 1, the impact of the transistor characteristics becomes more pronounced (Fig. 12).

5. Magnetic Materials. Choice of the magnetic material for power transformers affects efficiency and mass. It was found that out of the existing materials, the Permalloy appears best suited for the job. Details related to the choice of magnetic materials are given in Appendix A.

IV. CONCLUSIONS AND RECOMMENDATIONS

A. Conclusions

A power processor configuration that satisfies the general requirements of the NEP spacecraft was identified and the impact of the environmental conditions evaluated. It appears that the proposed configuration can satisfy the stipulated requirements.

B. Recommendations

The following recommendations concerning the NEP system were identified as a result of this study:

- (1) The preferred TFE-source voltages are 23 V or higher.
- (2) Transistor forward voltage drop and switching time have a strong effect on power processor mass, thus low forward voltage, high-speed transistors should be used.

- (3) Although not presently available, magnetic materials that exhibit low losses at high frequencies, that have a high Curie point, and that can operate at 15- to 20-kG flux level are desirable. Such characteristics could contribute significantly to additional reduction of the power processor mass.
- (4) Electrical component packaging on the radiator should be further studied to reduce the area that is sensitive to meteoroid penetration and thus greatly reduce the meteoroid shielding mass requirement.
- (5) An experimental model of the proposed power inverter should be built and tested to verify the efficiencies, masses, and all the automatic operational aspects.

Table 1. Environmental conditions

Case No.	Radiator temperature, °C	Effective space temperature, K	Meteoroid protection?
1	100	150	No
2	100	250	
3	50	150	
4	50	250	
5	100	150	Yes
6	100	250	
7	50	150	
8	50	250	

Table 2. TFE unit sources, characteristics

Voltage, V	Output		Number of TFEs in series (at 4V each)	No. of parallel strings (at 1A each)
	Voltage, V	Power, kW		
8		10	2	5
23		6	6	1
40		10	10	1

Table 3. Number (N) of TFE-source/inverter modules

TFE unit		N ^a
Voltage, V	Power, kW	
8	4	42
23	6	28
40	10	17

^aIncludes 20% redundancy.

Table 4. NEP power conditioner, power, efficiency, and losses
(for specific impulse of 4000 s)

Item No.	Power supply	Type	Output (rated), W	Estimated efficiency, %	Losses, W
1	Main vaporizer	ac	25	82	2
2	Cathode vaporizer	ac	25	82	2
3	Cathode heater	ac	50	80	10
4	Main isolator heater	ac	20	80	4
5	Neutralizer heater	ac	35	82	2.8
6	Neutralizer vaporizer	ac	20	82	1.6
7	Neutralizer keeper	dc	25	80	5
8	Cathode keeper	dc	50	82	4
9	Discharge	dc	900	94	54
10	Accelerator	dc	50	80	10
11	Beam (screen)	dc	4000	97	120
	Logic and harness		-	-	60
	Total		5200	95	275.4

Table 5. Efficiencies for different sources

Source voltage, V	Efficiency	
	Inverters and distribution, %	Power processor, %
8	94.13	89.42
23	94.48	89.75
40	95.34	90.57

Table 6. Assumed power transistor characteristics^a

Type	$E_{CE\ sat}$, V	T_{sw} , μs
A	0.1	5.0
B	0.4	0.75
C	0.7	0.75

^aRef. Figs. A-2, A-3, and A-4.

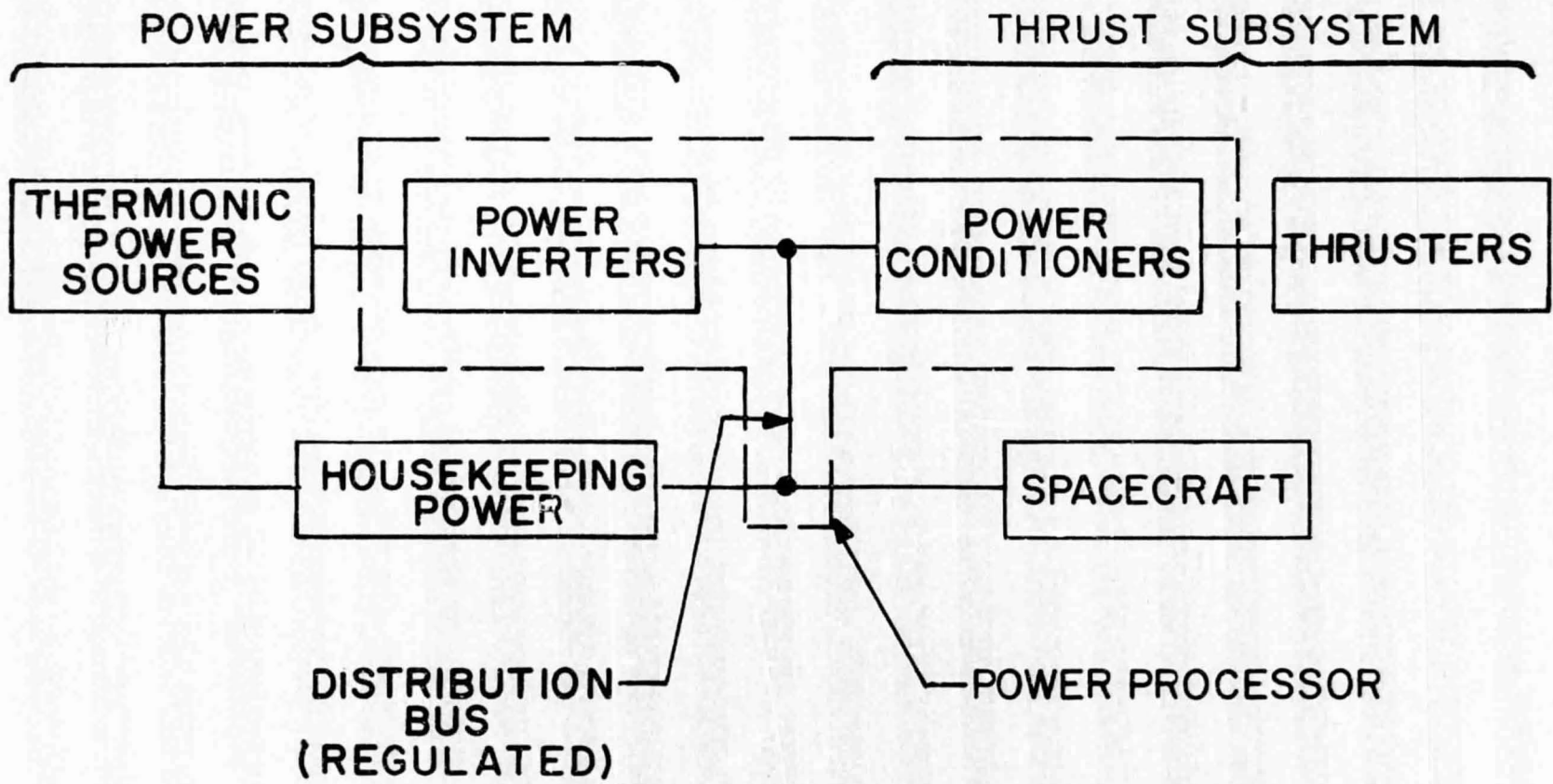


Fig. 1. Nuclear electric propulsion power processing configuration

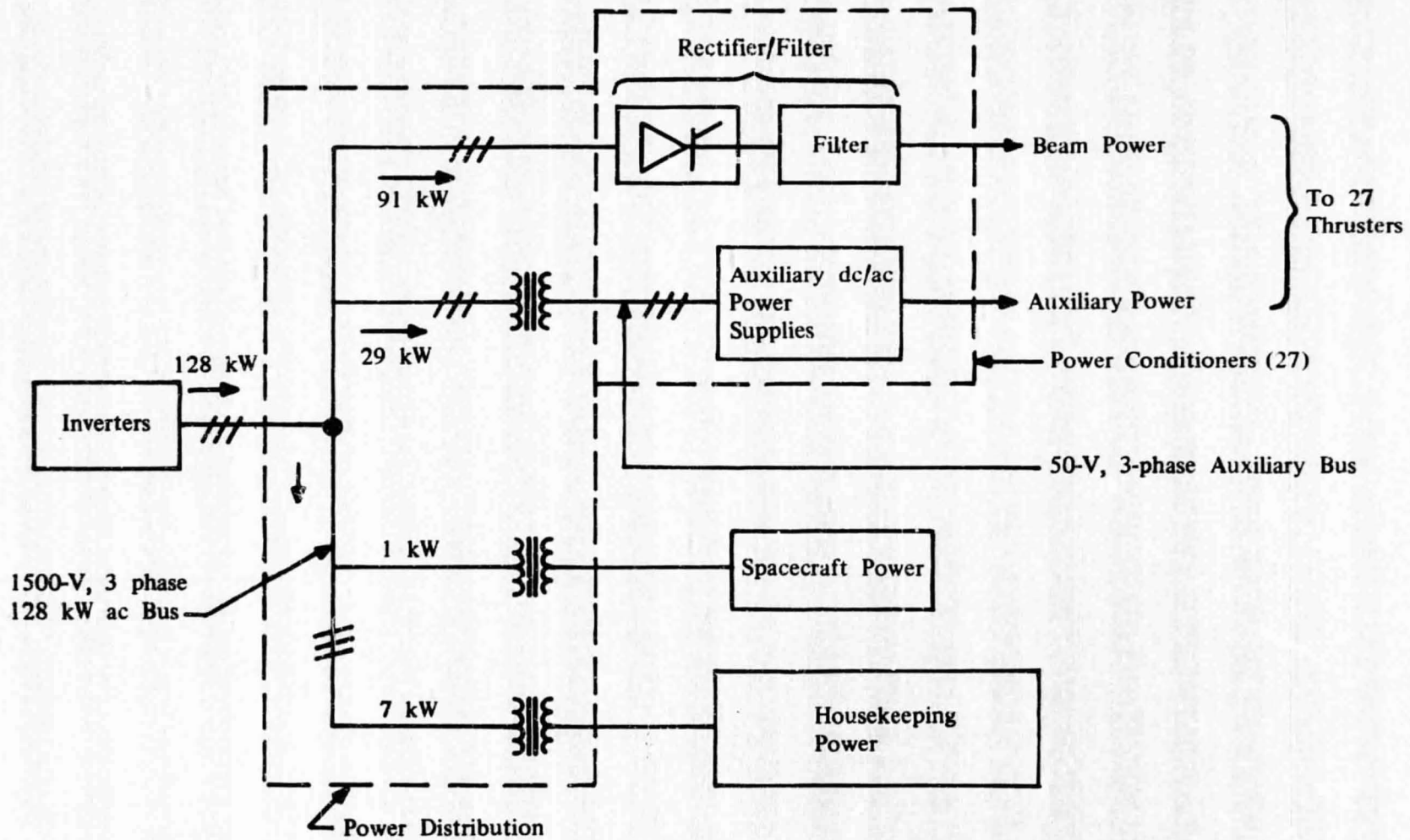


Fig. 2. Power distribution from ac bus to loads

Note: Ratings and designations as per Table 4

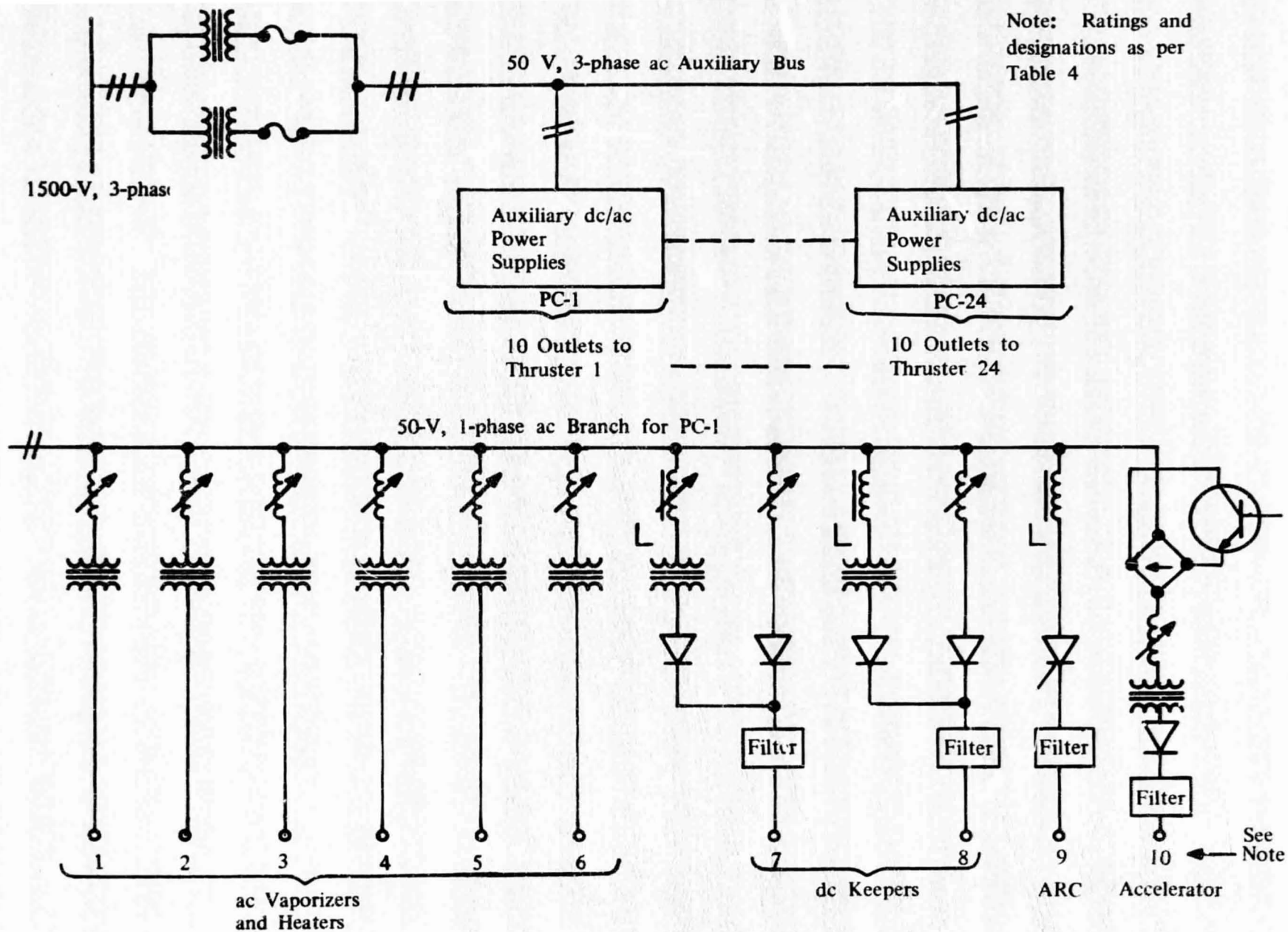


Fig. 3. Auxiliary thruster power distribution

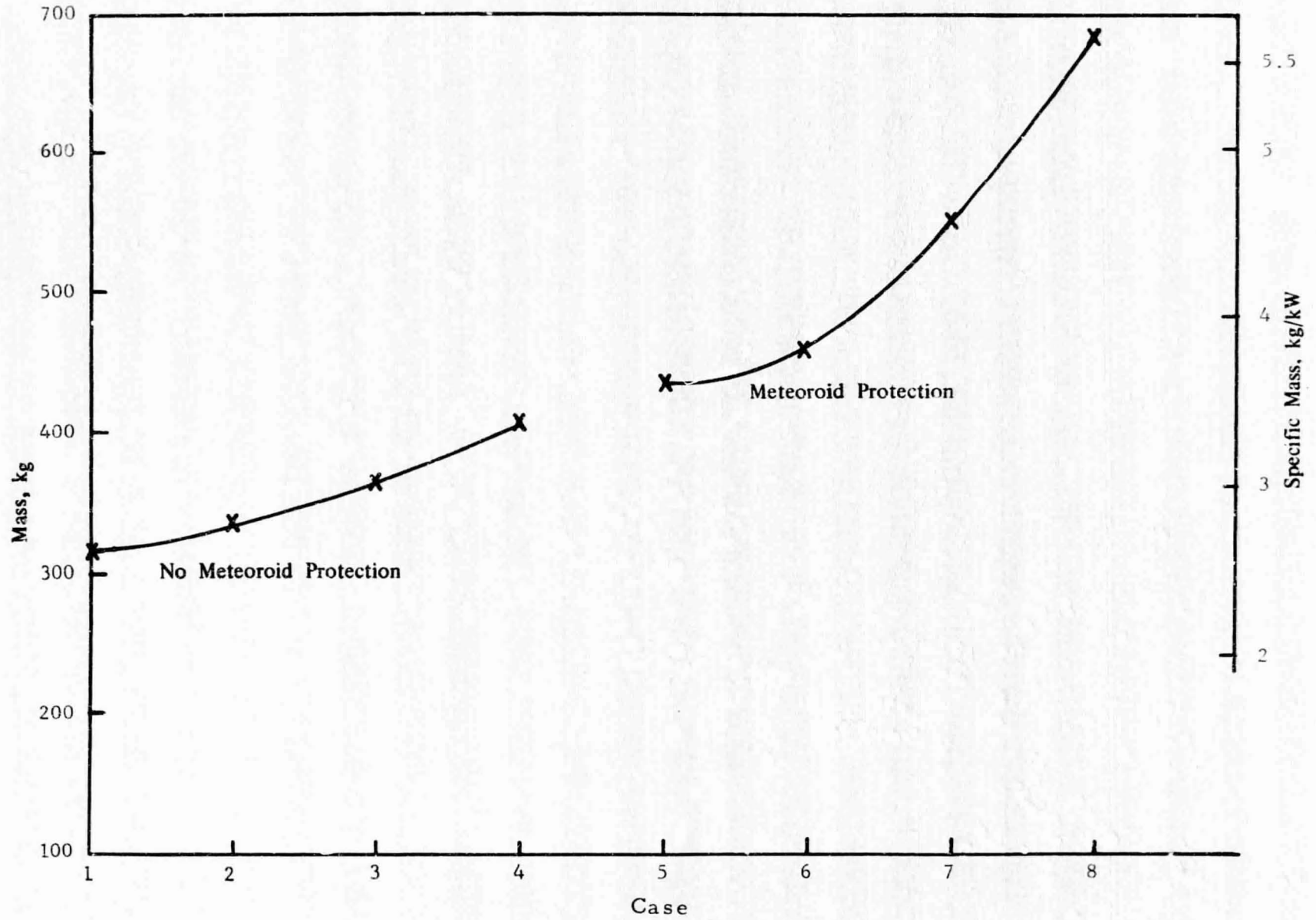


Fig. 4. Mass of radiators vs environmental conditions

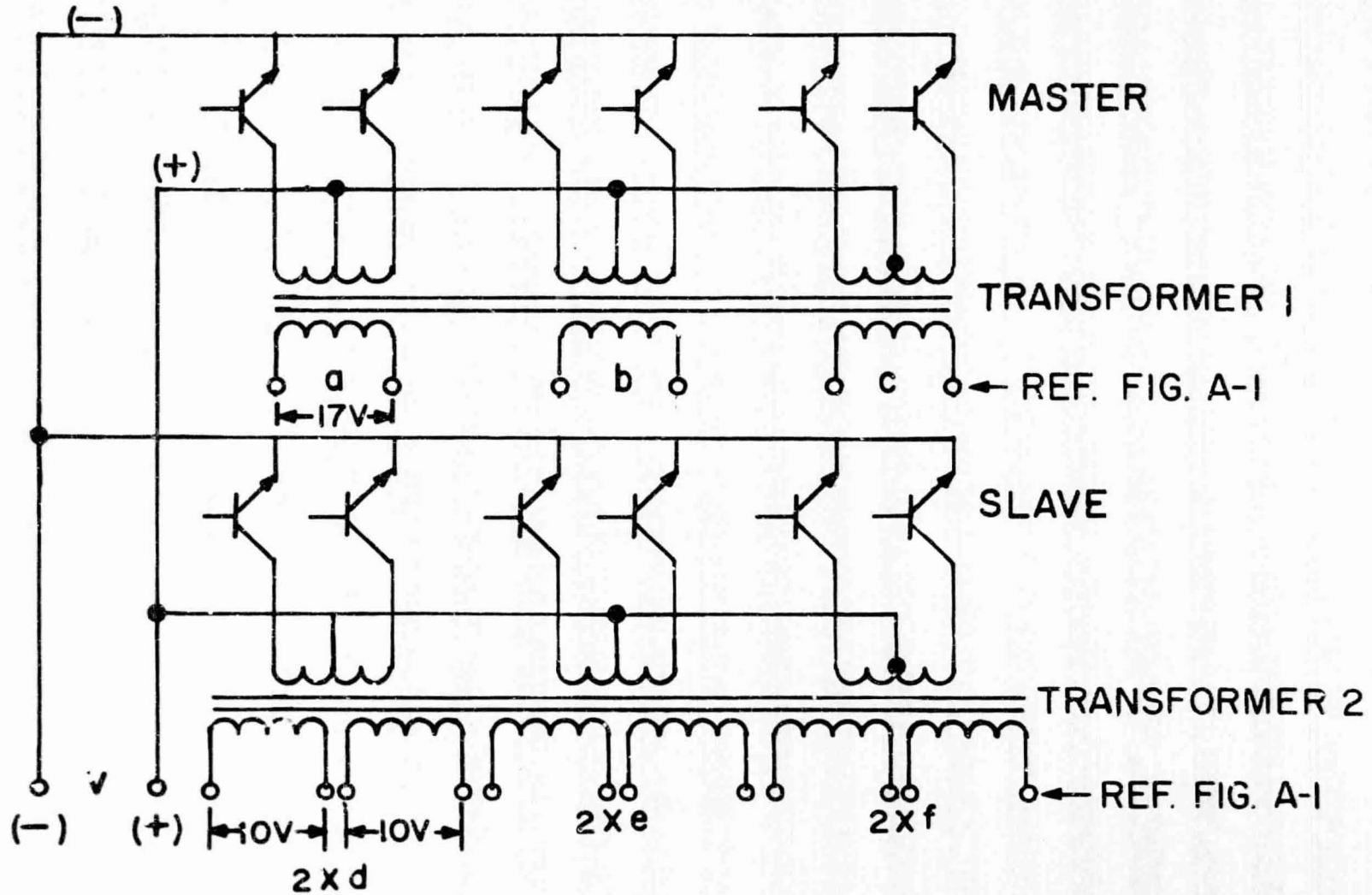


Fig. 5. Regulated power inverter, 3 phase

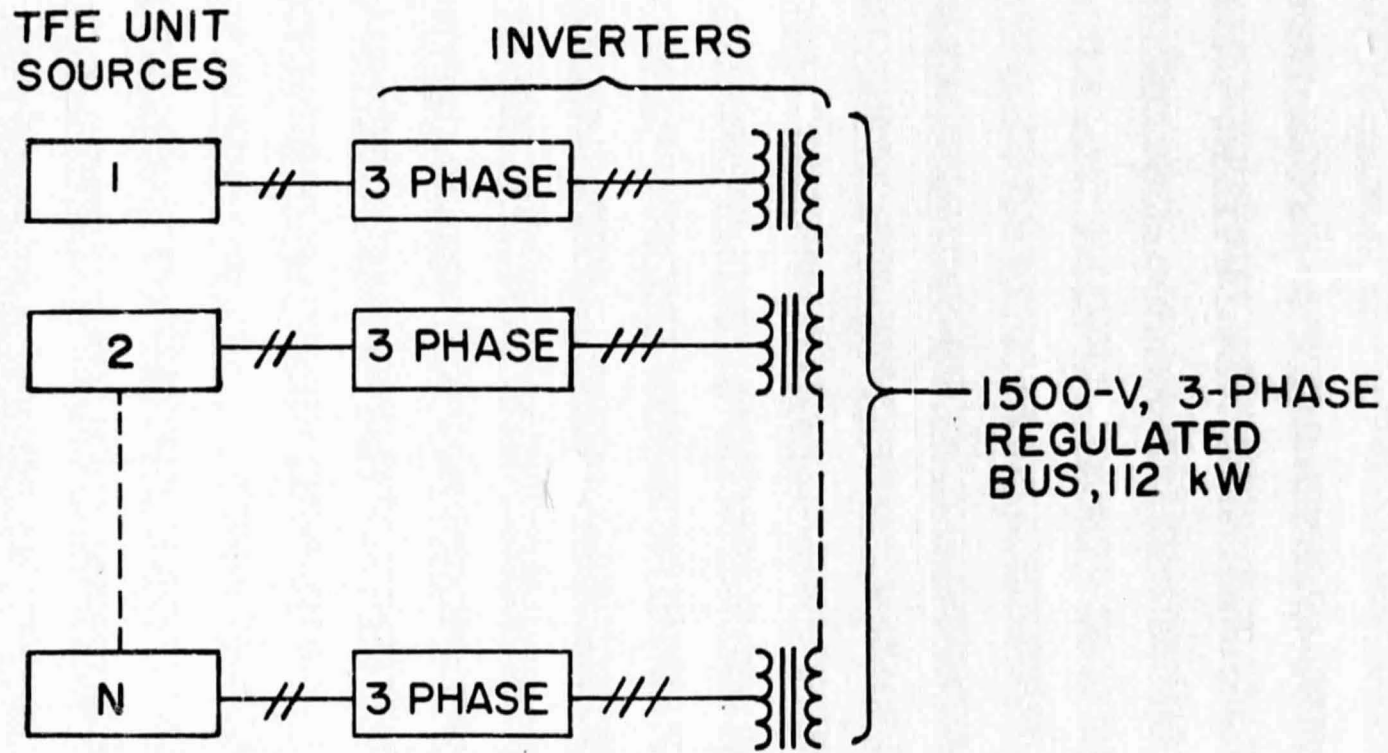


Fig. 6. Power subsystem, N modules

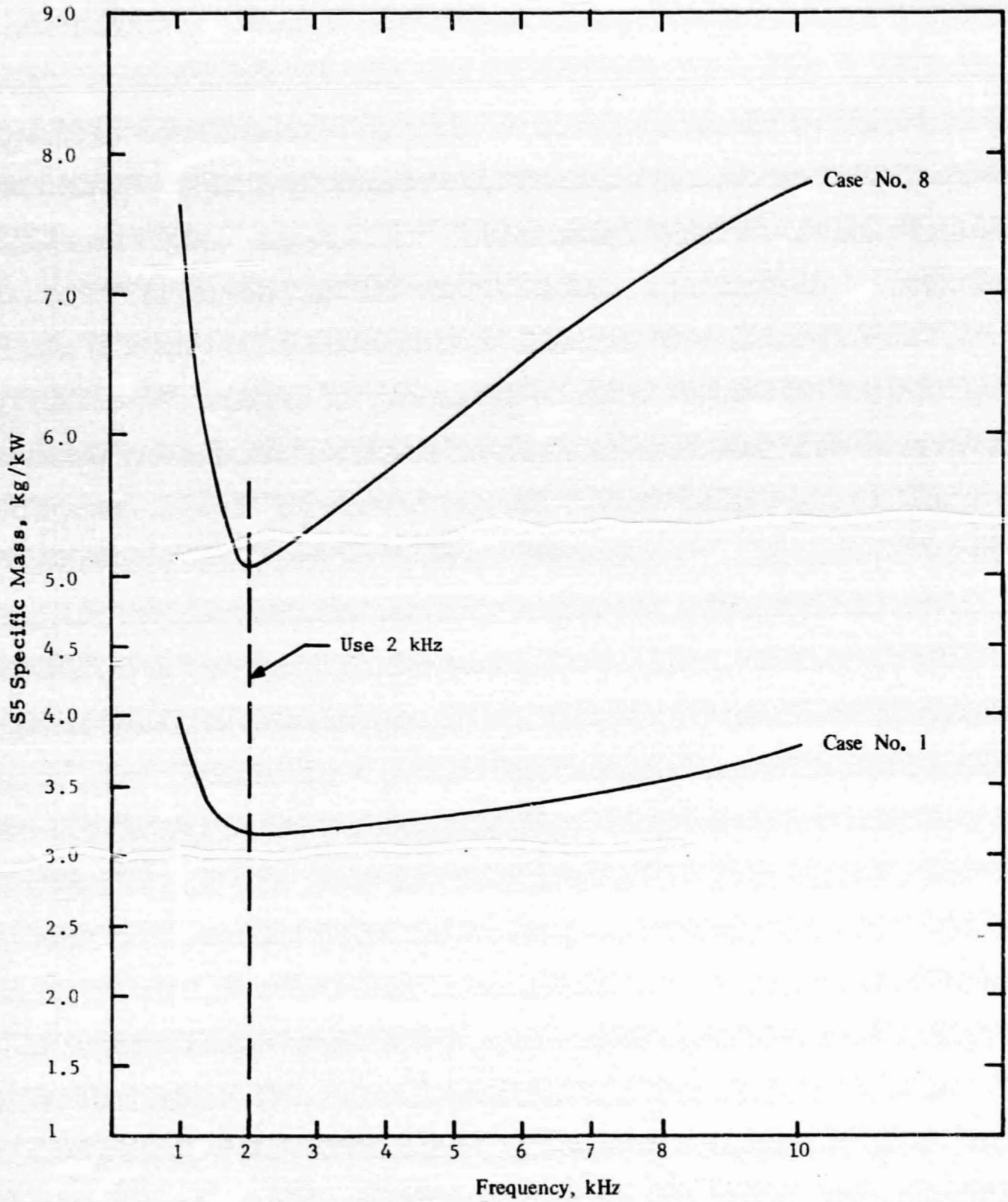


Fig. 7. S5 specific mass, 8-V source, inverter plus radiator plus source mass penalty

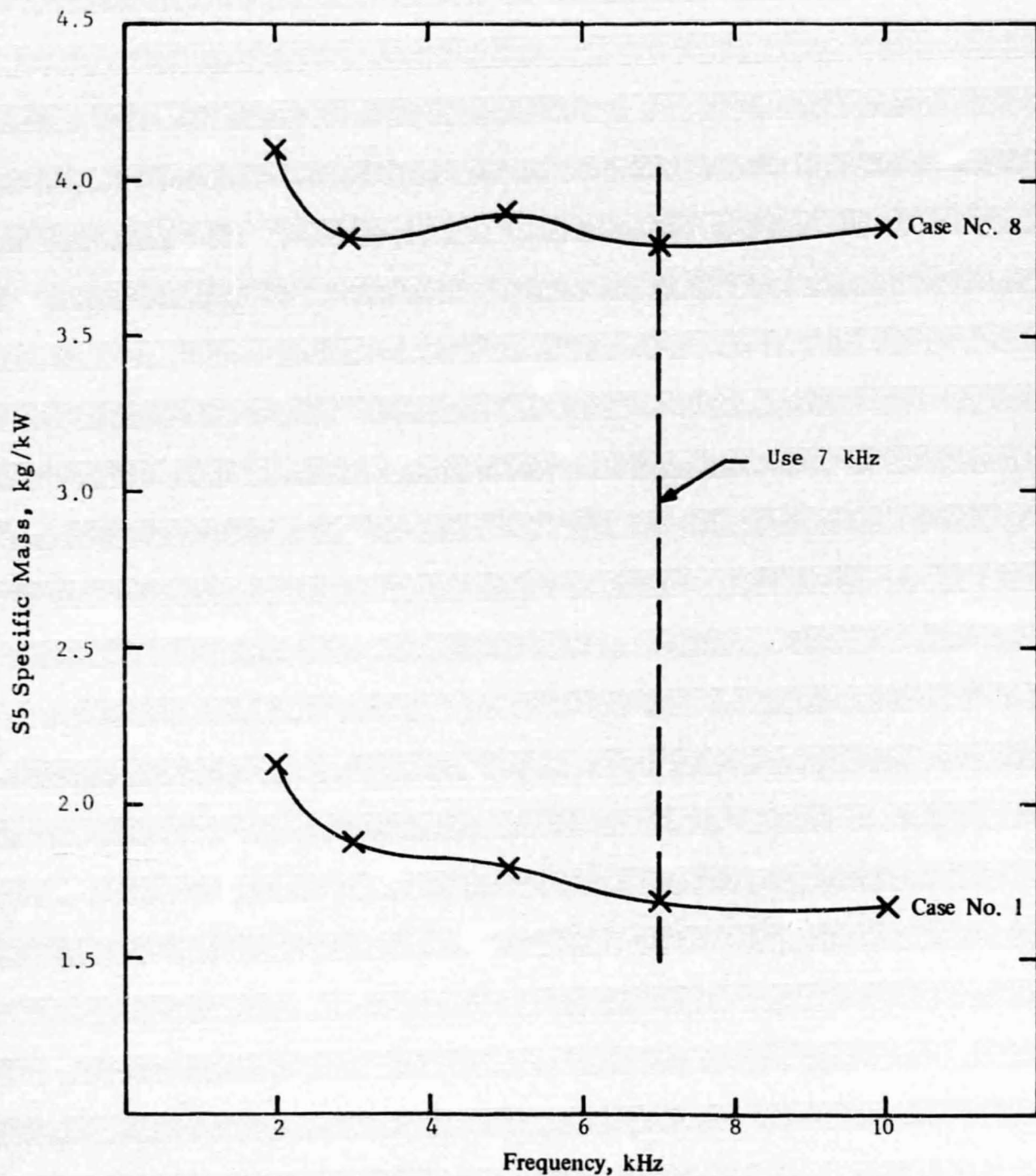


Fig. 8. S5 specific mass, 23-V source, inverter plus radiator plus source mass penalty

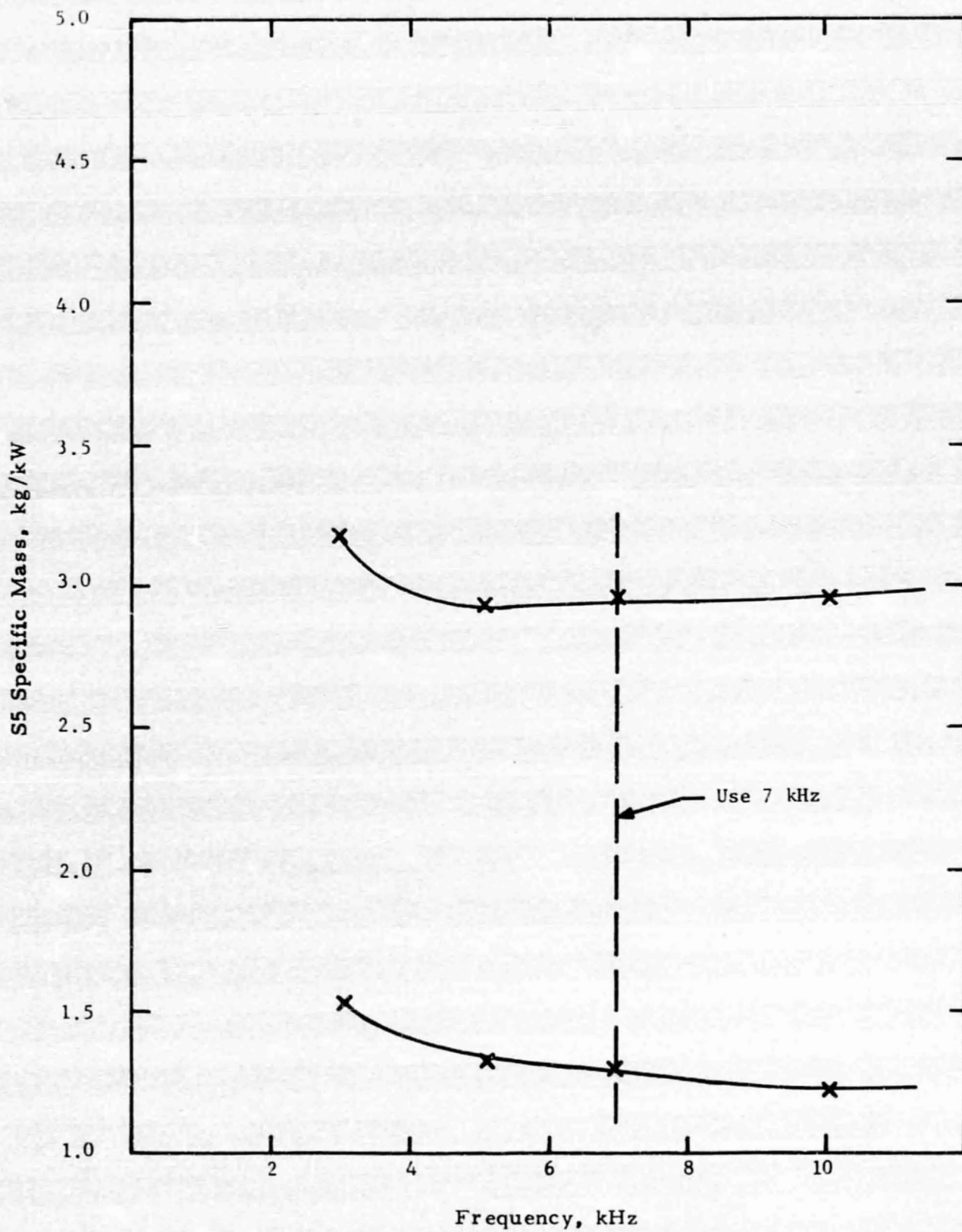


Fig. 9. S5 specific mass, 40-V source, inverter plus radiator plus source mass penalty

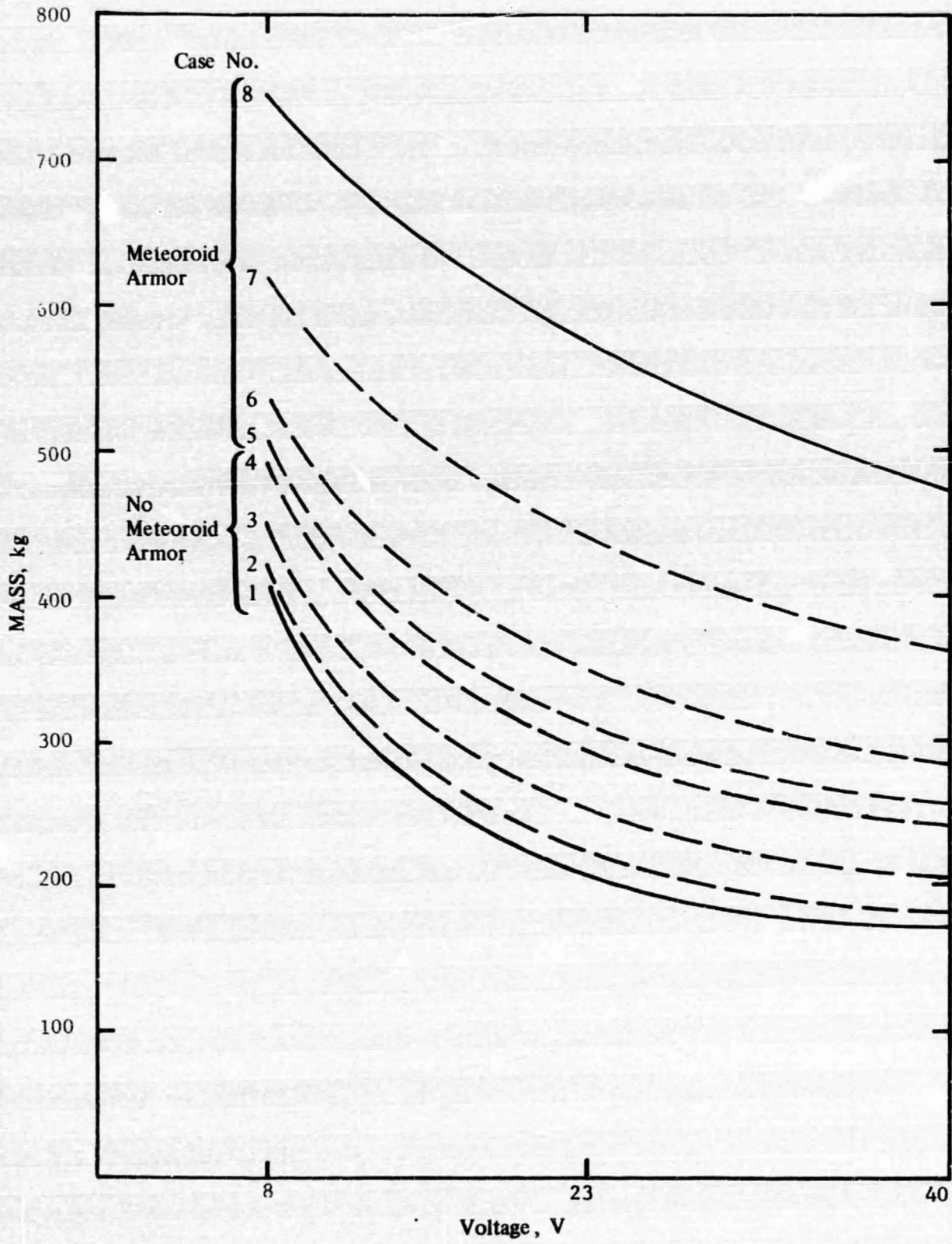


Fig. 10. Mass of inverters and distribution cables for various source voltages

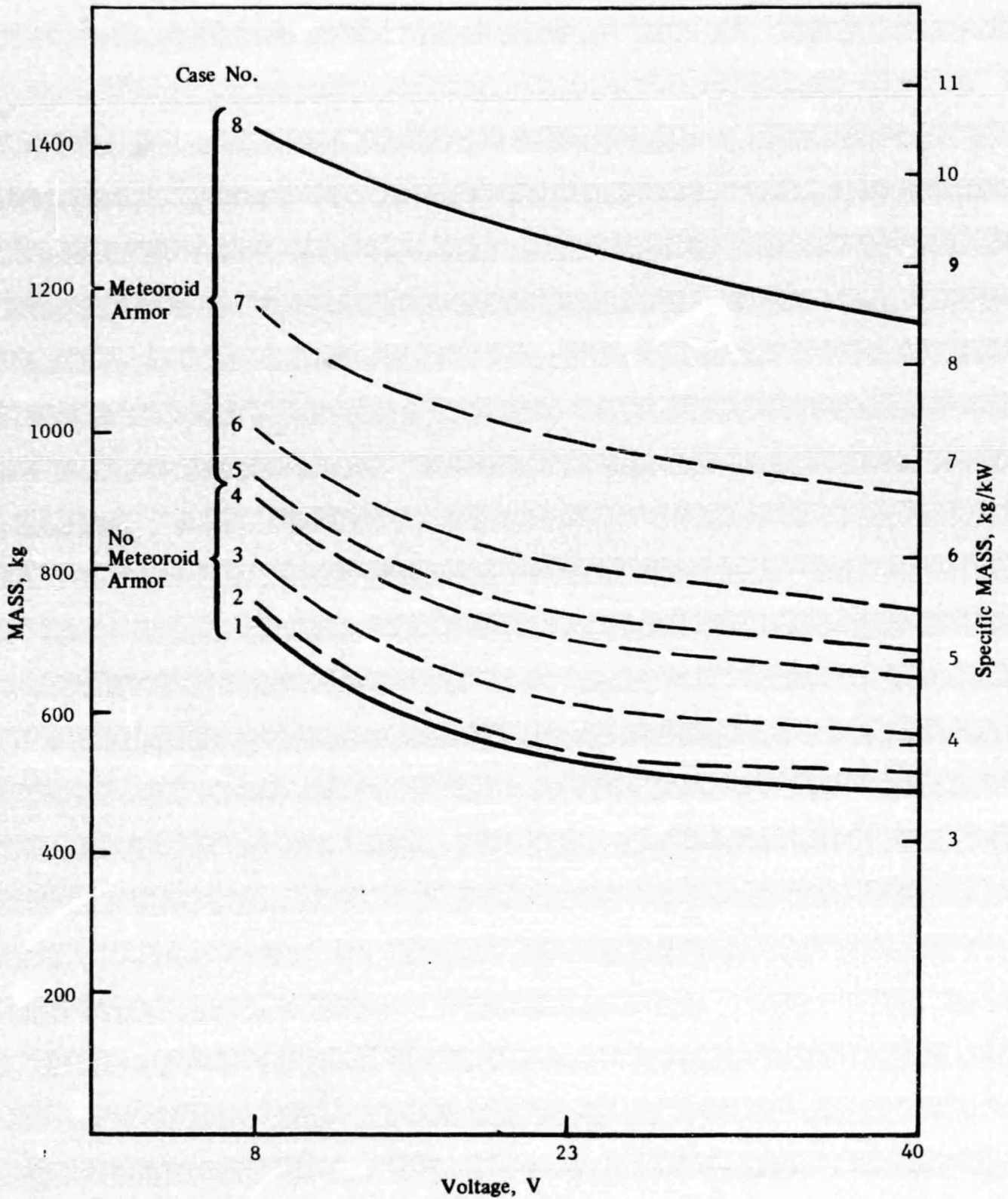


Fig. 11. Mass and specific mass power processor for different source voltages

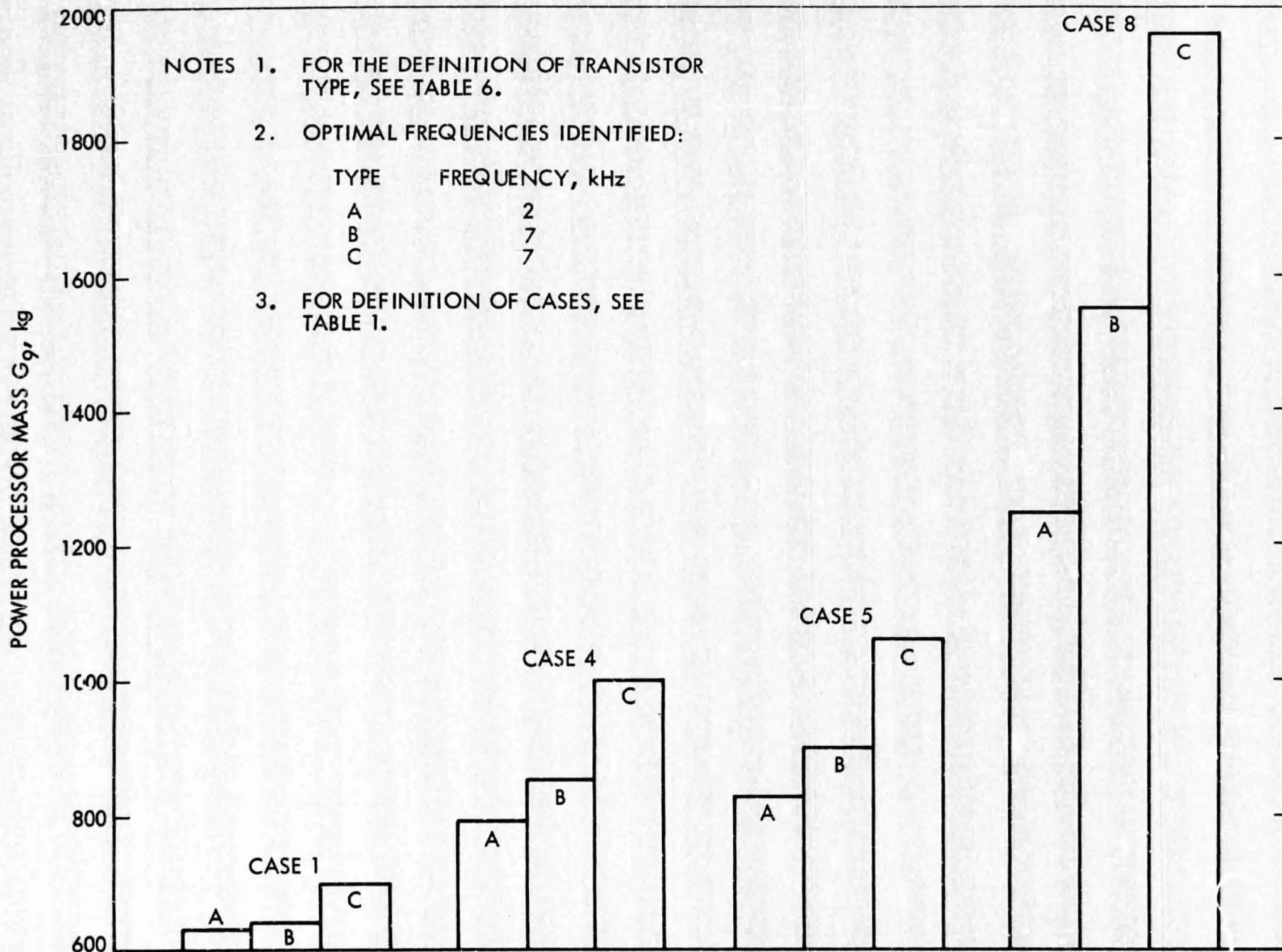


Fig. 12. Variation of mass of power processor with 8-V source for various transistor types

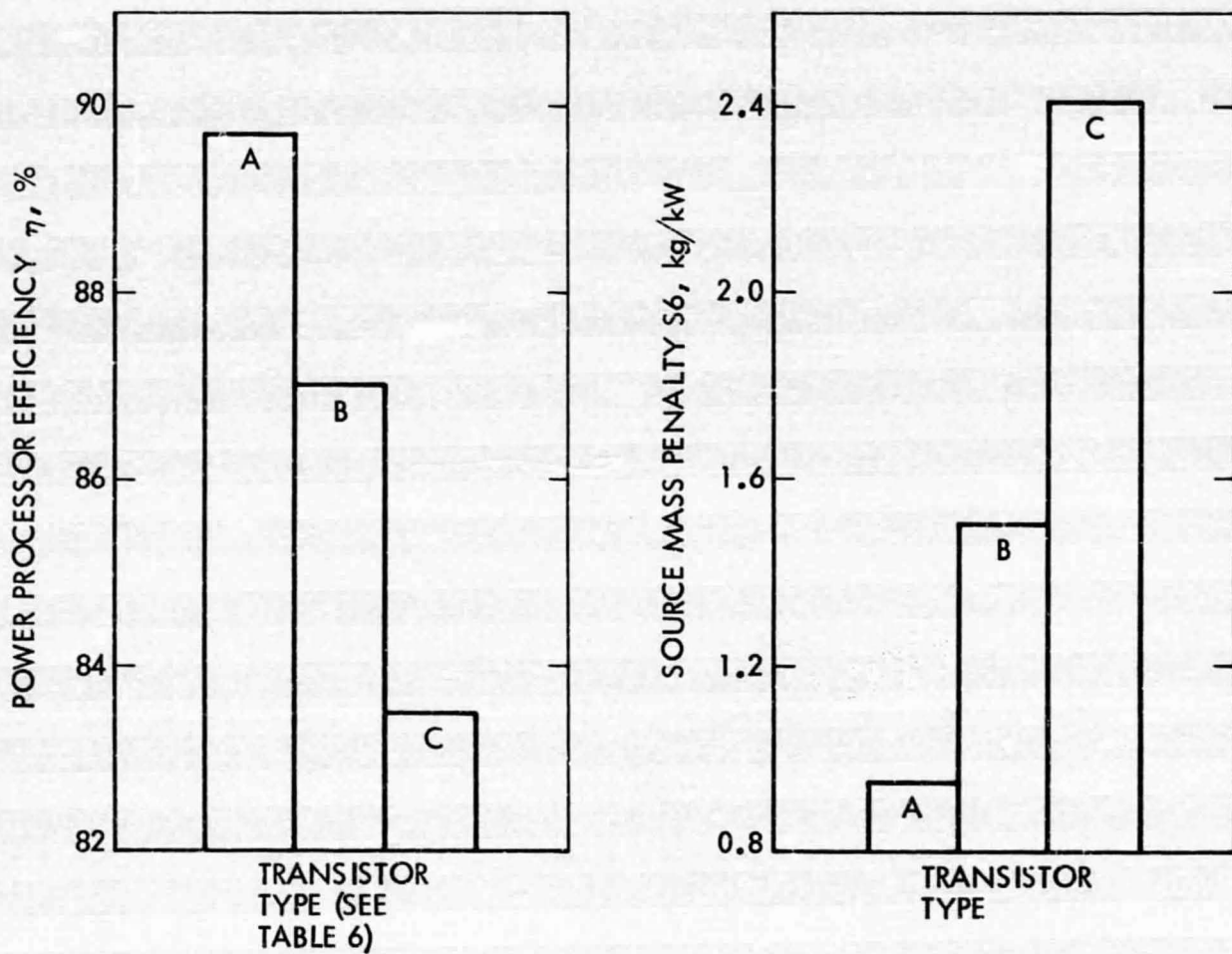


Fig. 13. Variation of efficiency and source mass penalty of power processor with 8-V source for various transistor types

APPENDIX A POWER CONVERSION

A. Inverter Configuration

The dc-to-ac power conversion is accomplished by a tandem-type inverter (Fig. 5). Two three-phase inverters, a master and a slave, drive two separate three-phase transformers. The two transformer outputs are interconnected in a star-zig-zag configuration to produce a three-phase, ac output voltage (Fig. A-1). If the individual phases of the slave unit are delayed by 30 electrical degrees with respect to the corresponding phases of the master unit, all harmonics below the 11th are eliminated. The resulting ac output voltage is nearly sinusoidal, which improves the electromagnetic compatibility and reduces the electrical losses. The amplitude of the output voltage is controlled by pulse-width modulation, details of which can be found in Section C below.

B. Critical Components

1. Transistors. For the purpose of this study, two types of power transistors were considered (Table 6). Both of them are, at the time of writing, "specials". Type A has been developed for JPL by Westinghouse (Ref. 4); Type B represents the state-of-the-art transistor of today.

For comparison, another type, Type C, which represents today's commercially available transistor, was considered. Type C was, however, used only to generate the data on Figs. 12 and 13 to show how much the choice of the transistor can affect the overall design. The parameters of interest to the study are listed in Table 6. For the purpose of this study, the mass of a power transistor and the driving transistor, complete with the mounting hardware, was assumed to be 150 g. The number (M) of transistors per inverter module is 24 for the 8-V configuration and 12 for the 23-V and 40-V systems. The following equations (Ref. 5) were used to evaluate the transistor losses:

$$\text{Saturation losses: } P_{\text{sat}} = \frac{M}{2} \times I_C \times E_{\text{CE sat}}$$

$$\text{Switching losses: } P_{\text{SW}} = \frac{4M}{9} \times V \times I_C \times T_{\text{SW}} \times F1 \times 10^{-3}$$

The definition of the symbols used can be found at the end of this report.

The graphical plot of the sum of saturation and switching transistor losses vs frequency is shown in Figs. A-2, A-3, and A-4. The choice of the type of device used depends upon the operating frequency; the transistor that offers minimum loss is chosen.

2. Output Transformers. Two three-phase transformers are used in the inverter's output. Cores are of standard three phase "E" type, per Ref. 6. These cores are available in a wide range of core sizes. The use of "E" cores permits the building of very compact three-phase transformers, which are smaller and lighter than similar units, using three, single-phase cores Fig. A-5.

Various types of magnet steel were considered. The Supermendur, with grain-oriented 50% iron, 50% cobalt material, and 20 kG flux density, was found excellent below 1 kHz. The Orthonol did not quality. Ferrites were not considered because of the nonavailability of cores in the large sizes. The 2-mil Permalloy (80% Ni, 20% Fe) was chosen because it is best suited for the frequency range investigated. The core loss curves for the 2-mil Permalloy are shown in Fig. A-6. Flux density was chosen as 6.5 ± 1 kG. Each coil consists of two windings: a center-tapped primary winding, and single or double secondary winding.

Coils would be wound using standard copper wire sizes with Class H, high-temperature insulation. An electrostatic shield would be inserted between the two windings to eliminate the high-frequency coupling. To take care of the detrimental skin effect, the individual coils would use multiple parallel wires. The penetration depth (p) of the current with good approximation can be derived from:

$$p = \frac{2.61}{\sqrt{f \times 10^3}}$$

Results are presented in Table A-1. Based on the results, we find that, for an operating frequency of 5 kHz, the largest acceptable wire size is 13 AWG. Use of the wire size 12 AWG would add to the mass without

reducing the current density. The single wire sizes required are, generally speaking, in the vicinity of a number 8 AWG. Because of redundancy and reliability requirements, multiple wires are used for the individual coils. The equivalent active cross section of the 8-AWG wire can be obtained by using two 11-AWG, four 14-AWG, or eight 17-AWG wires in parallel.

The current density was limited to 2500 A/in.^2 . Densities above that value were not considered. A 20% safety margin was added to calculated transformer losses for unaccounted losses. Losses in the inverter harness and connectors were estimated at 1%.

The calculated mass of iron was increased by 20% to account for the mounting hardware and support structure.

C. Controls

The average and rms value of the square wave of a constant amplitude (Fig. A-7) can be varied by reducing the half-cycle conduction time from $T/2$ (Case 1, Table 1) to $(T/2 - d)$ on both the master and the slave. The 30-deg offset between the master and slave remains unaffected by the value of d . The same applies to the relative average/rms value of the master and slave.

To keep the output voltage constant, the angle d must be controlled by an error voltage feedback. The feedback mechanism reduces the non-conducting time when the input voltage drops and increases the nonconducting time when the input voltage increases.

The weight of the control logic module and auxiliaries was estimated as 700 g per inverter module.

Table A-1. Skin effect penetration depth (p) and AWG-wire size for different frequencies

F1, kHz	AWG	p , mils
1	6	82
5	13	37
10	17	26
15	18	22

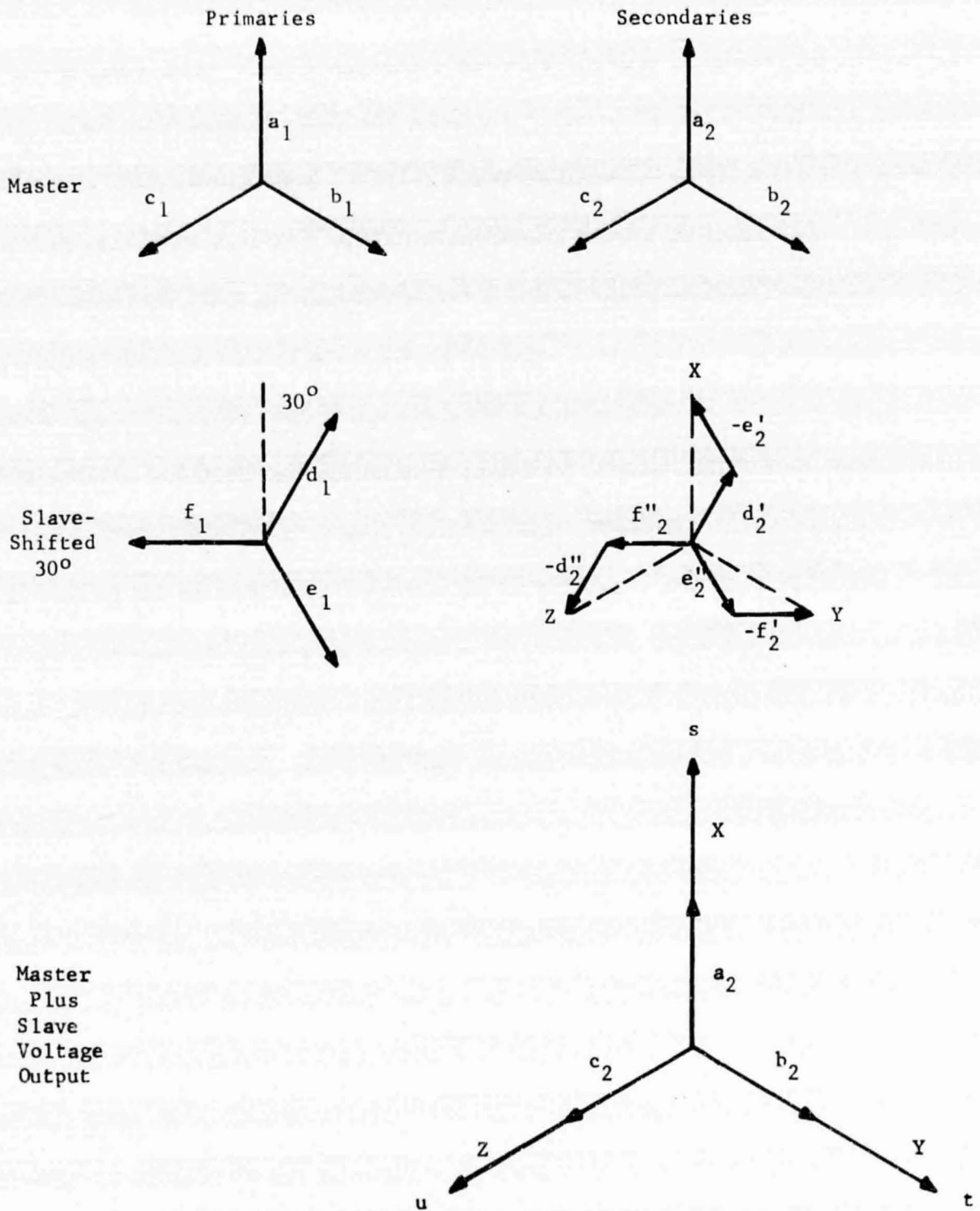


Fig. A-1. Input and output voltages, power inverter module

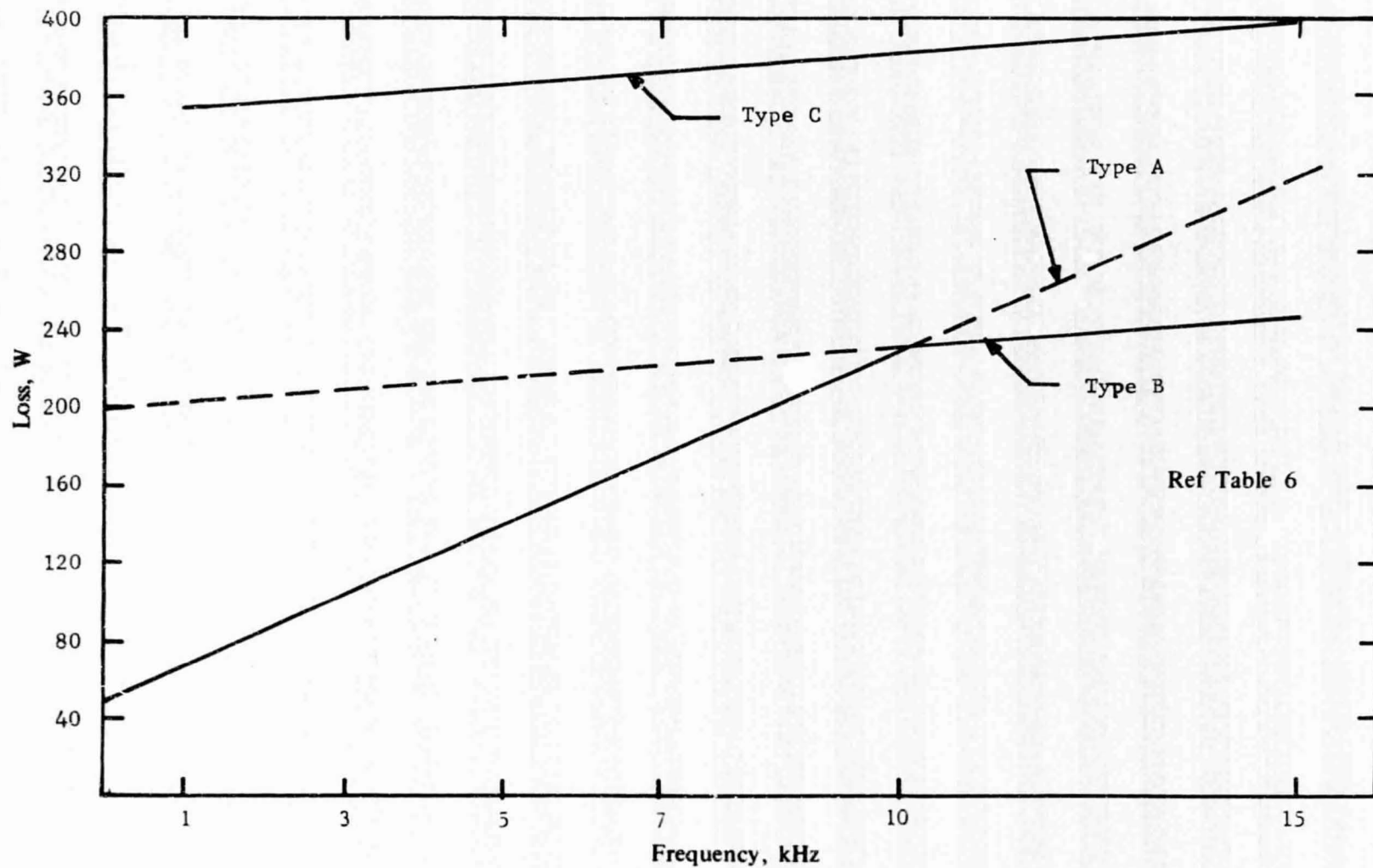


Fig. A-2. Transistor losses for three types of transistors, 8-V power inverter

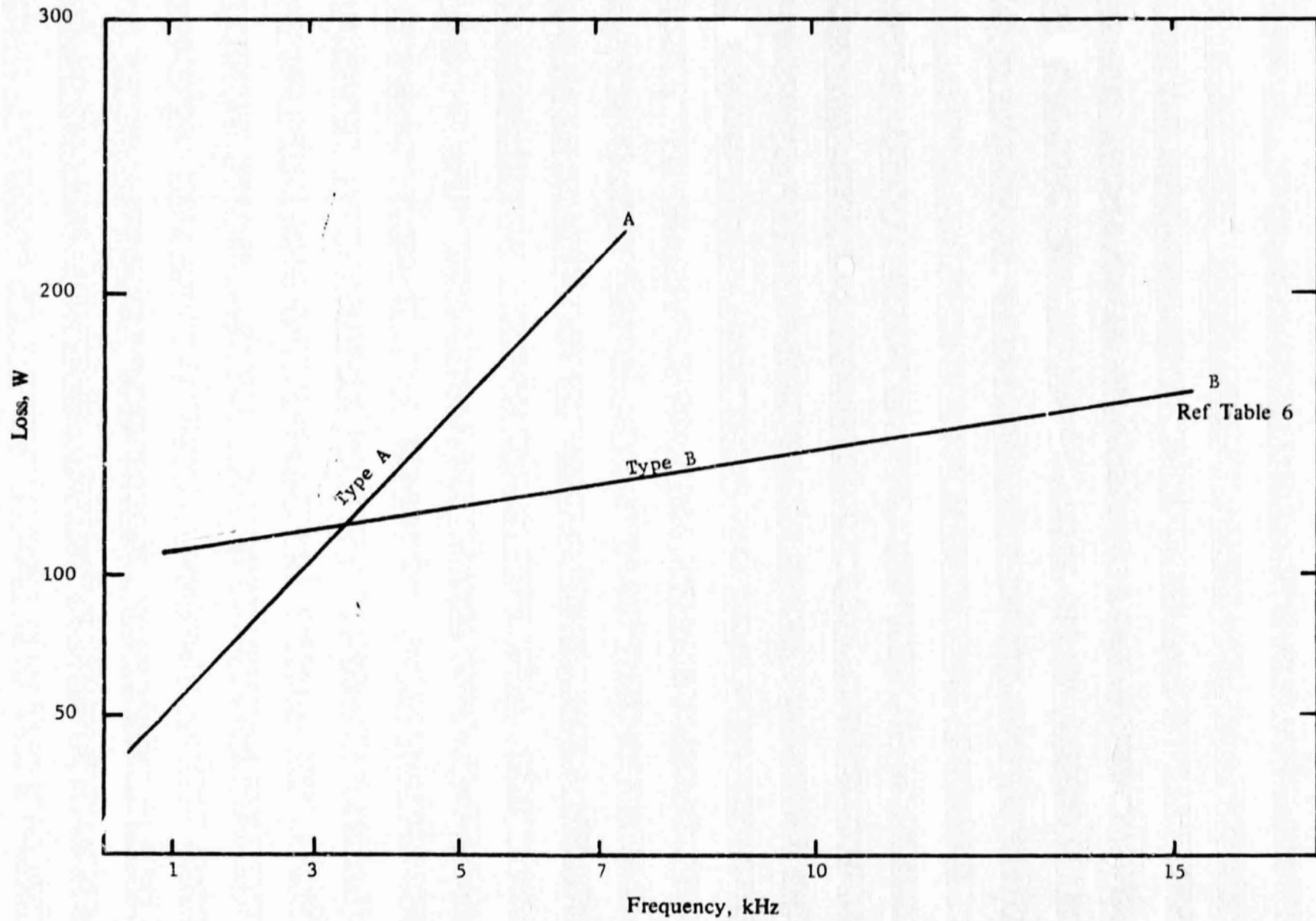


Fig. A-3. Transistor losses for two types of transistors, 23-V power inverter module

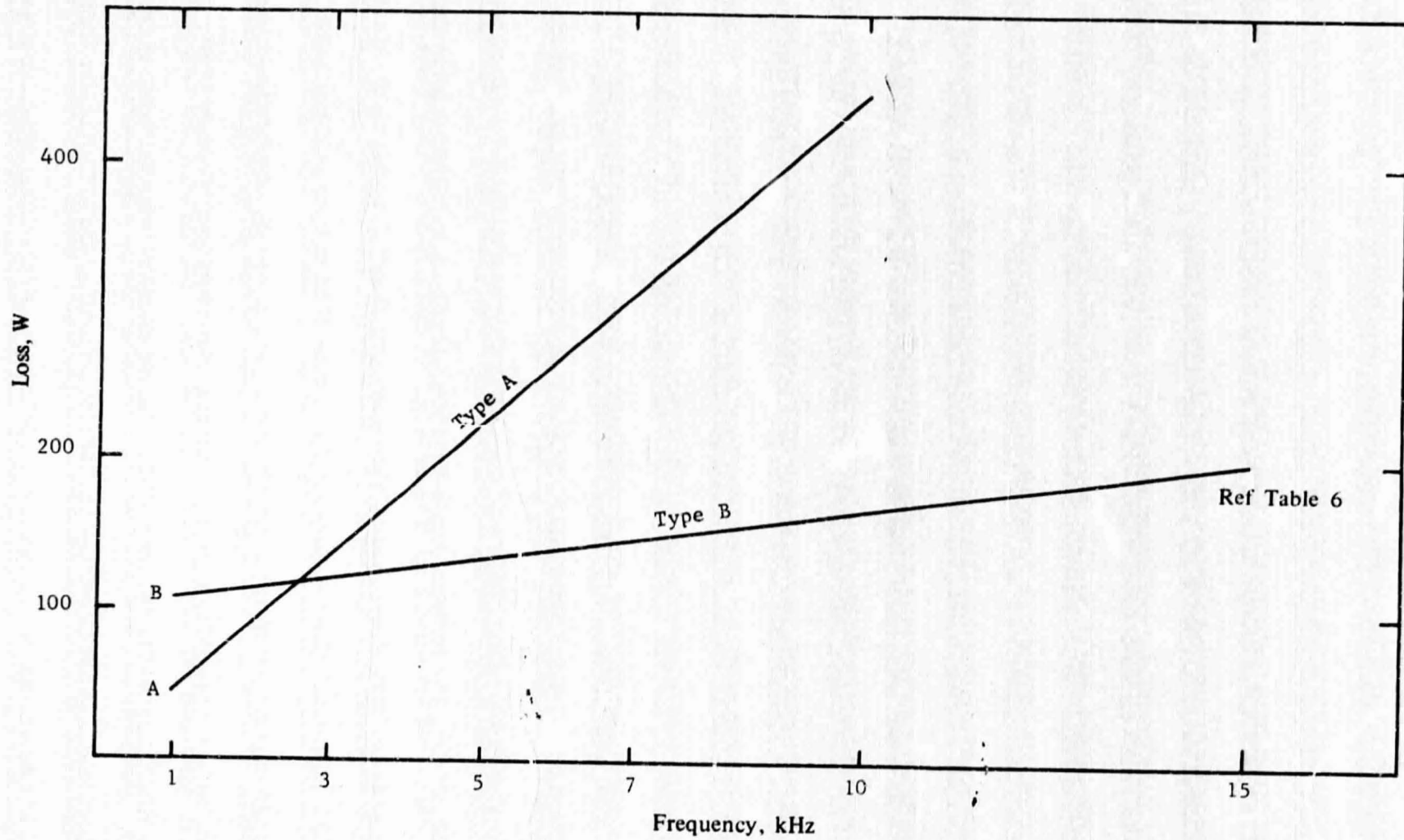


Fig. A-4. Transistor losses for two types of transistors, 40-V power inverter module

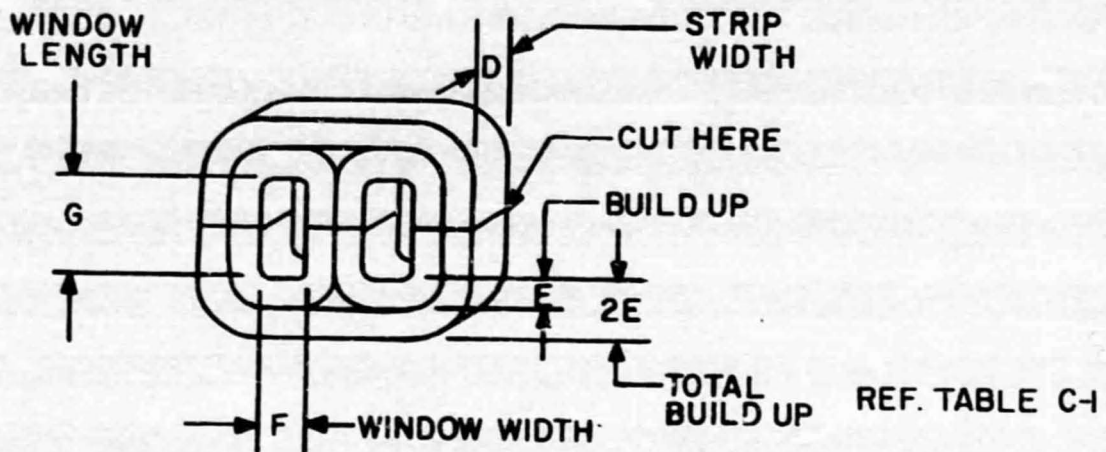


Fig. A-5. Core dimensions

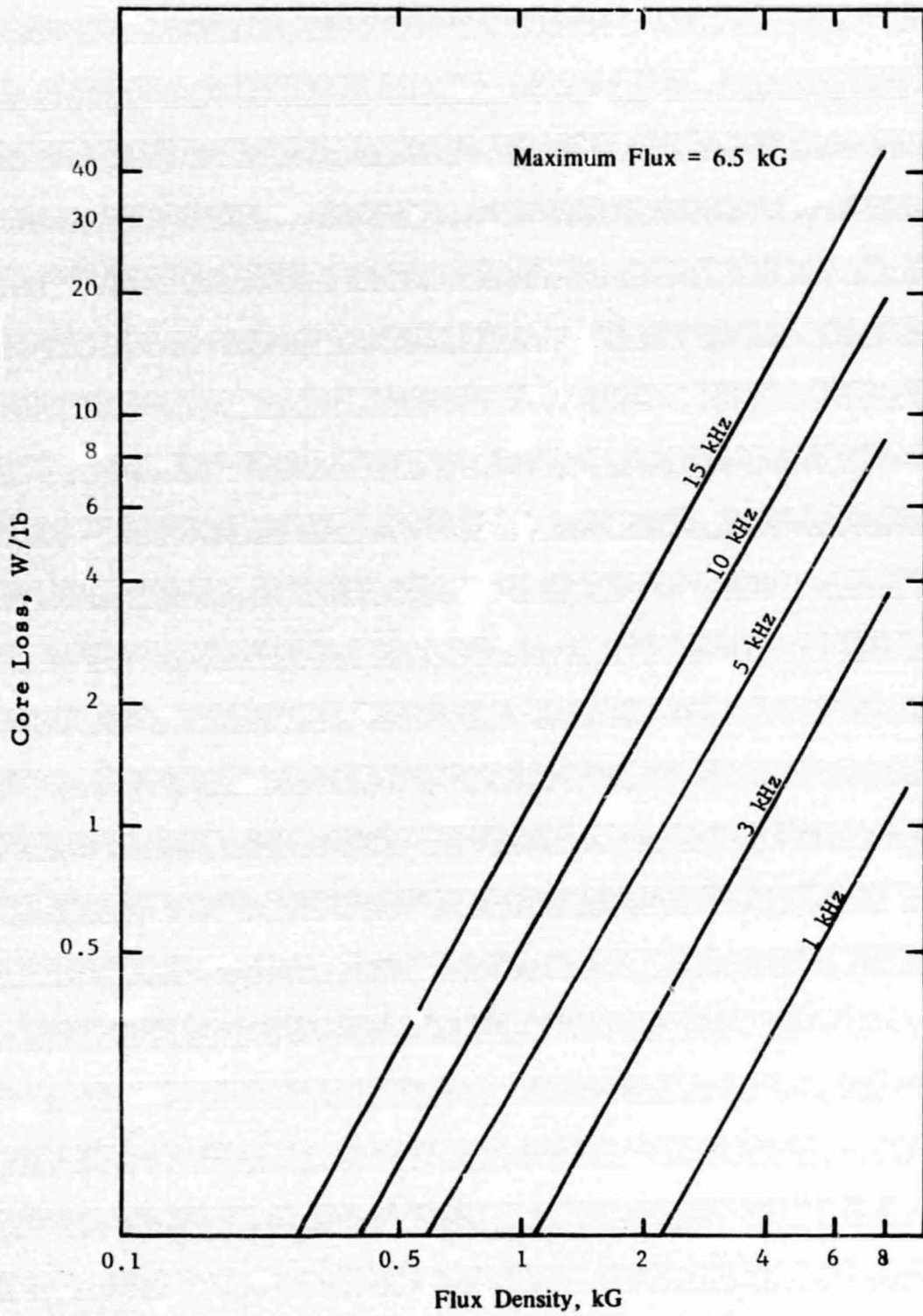


Fig. A-6. Core loss curves, 2-mil Permalloy

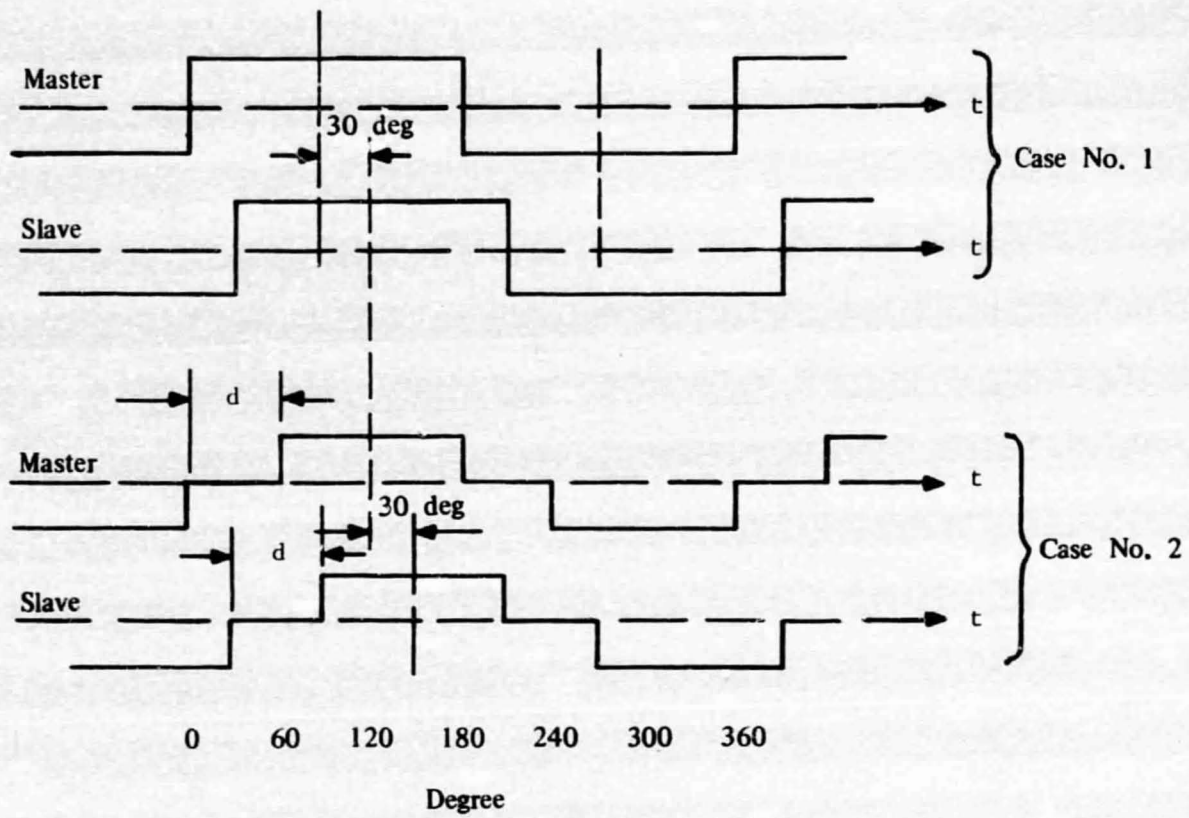


Fig. A-7. Power inverter output voltage control

APPENDIX B

RADIATORS

The radiators were designed to reject the heat generated in the semiconductors, magnetics, harnesses, and cables. The radiator was required to support the power processor components, survive the launch, and protect the components from any meteoroid impacts. The radiator panels were designed with all components of the power processor mounted on one side of the panel. The radiator consisted of an aluminum alloy structure, subdivided by I-beams with module flat-plate radiators inserted into each opening.

For the analysis, each panel was assumed to be 0.5 m wide by 2 m long. The structure was assumed to consist of 5 I-beams that divide the 2-m length into 6 equal modules, with a light aluminum frame around the periphery. Other smaller beams would be required to further divide the panel into electrical modules, but these beams were not included in the analysis.

To keep the electronic module flexing amplitudes within acceptable limits during launch vibration, the panel's first mode natural frequency was maintained below 200 Hz. Based on the curves in Ref. 7, the 0.5-m I-beams were sized for a cross-sectional stiffness (EI) of $6 \text{ kN}\cdot\text{m}^2$. The mass of such beams was about 0.6 kg/m. The peripheral frame was assumed to have a mass of 0.3 kg/m. The individual panels were mounted on the cylindrical surface of the spacecraft. For simplicity, it was assumed that the entire cylindrical surface was isothermal, and this led to an effective sink temperature estimated at 150 K (or 250 K for geocentric missions).

The radiator's thickness and, consequently, mass varies with the level of the meteoroid protection required. Two extreme cases were considered, one where there was no meteoroid protection, and the other where protection was provided.

The armor thickness was based on the Mariner-Jupiter-Saturn (MJS) asteroidal meteoroid flux model. Recent preliminary data from the flight of Pioneer 10 (Ref. 8) indicate that the MJS model may be ultraconservative.

For the analysis it was assumed that particles of mass less than 0.003 (0.12-cm diam) must be stopped. This corresponds to a 0.99 probability of no penetrations per square meter of radiator surface. Consistent with single-sheet penetration theories, the aluminum shear plate thickness was assumed to be five times the diameter of the largest meteoroid to be stopped, or, in that case, 6 mm. In the first case, the radiator mass was estimated to be 6.5 kg/m²; in the second case, 20 kg/m².

The radiator area requirements were dictated by the temperature differences between the temperatures of the radiator and the sink (i. e., equivalent space sink temperature). This study considered two temperatures, 50 and 100°C, for the radiators. Similarly, two effective sink temperatures (T₀), 150 and 250 K, were used.

The effective sink temperatures caused by the solar irradiation at 90° incidence to the cylinder axis were derived from the equation:

$$T_0 = \left[\frac{s_1 \alpha}{\sigma \pi \delta^2 \epsilon} \right]^{1/4}$$

where

s₁ = solar irradiance at 1 AU, s₁ = 1353 W m⁻²

α = solar absorption of radiator coating

ε = emittance of radiator coating, α/ε = 1

δ = heliocentric distance, AU

σ = Stefan-Boltzman constant, as below.

The T₀ values represent the highest attainable value because the solar energy irradiation was assumed normal to the surface of the radiators.

The specific area, in m²/kW, was determined from the Stefan-Boltzman radiation heat transfer equation:

$$\frac{q}{A} = \sigma (T^4 - T_0^4)$$

where

q = power dissipation, W

A = area, m^2

T = radiator temperature, K

T_0 = effective sink temperature, K

σ = 5.6697×10^{-8} , $\bar{w} m^{-2} K^{-4}$

ϵ = emittance 0.85

The product of the specific structural mass in kg/m^2 and the specific area in m^2/kW defined the radiator specific mass (S7) in kg per kW of power processor electrical losses. Table B-1 lists the radiator specific mass for the eight cases considered. These values were used to determine the radiator required to cool the power inverters, power distribution cables, and power conditioners.

Table B-1. Radiator specific mass

No meteoroid protection	
Case No. ⁱ	Specific mass, kg/kW loss
1	6.5
2	8.38
3	12.47
4	18.48
Meteoroid protection	
Case No. ^a	Specific mass, kg/kW loss
5	20.8
6	25.4
7	37.8
8	56.0
^a For definition of all eight cases, see Table 1.	

APPENDIX C
INVERTER DESIGN

A. Introduction

The design of the individual three-phase inverter module was programmed into the computer. It was assumed that the master and slave inverters were identical (Fig. 5).

B. Design Procedure

1. Preliminaries. All the symbols used here are listed at the end of this report.

The design starts by specifying the following parameters: F1, V, B, J, P7, and P6. The product

$$N1 * A1 = Z \quad (C-1)$$

will be found useful and, therefore, shall be specified in terms of a known parameter. From Fig. A-5:

$$A1 = K * D * 2 * E \quad (C-2)$$

From the fundamental equation:

$$V = 4 * F1 * N1 * A1 * B * 10^{-8}$$

After converting the international units to the practical units used, from the above:

$$Z = \frac{3.9 * V}{F1 * B} \quad (C-3)$$

The primary current rms first harmonic is:

$$I1 = Id / \sqrt{3} = 0.578 * P7 / V \quad (C-4)$$

The total window cross section is (Fig. A-5):

$$W = 2 * F * C \quad (C-5)$$

2. Copper Conductor Size vs Size of Window and Number of Turns.

In the three-phase configuration, three identical coils are employed. Only a $1/4$ -W area can be used for each coil (Fig. A-5). Because of practical considerations, 32% of that area was made available for the copper. That means

$$Q_C = 0.25 * W * 0.32 = 0.08 * W \quad (C-6)$$

Each coil consists of the primary and the secondary. Both, combined, occupy

$$Q_C = 2Q_{C1} + Q_{C2} \quad (C-7)$$

It can be proven, then, that

$$Q_{C2} = \sqrt{2} Q_{C1} \quad (C-8)$$

Therefore,

$$Q_C = 3.41 Q_{C1} \quad (C-9)$$

where

$$Q_{C1} = N1 * A2 \quad (C-10)$$

Coml ining Eqs. (C-6), (C-9), and (C-10),

$$3.41 * Q_{C1} = 0.08 * W$$

or

$$3.41 * N1 * A2 = 0.08 * W$$

and

$$W = \frac{N1 * A2}{0.0235} \quad (C-11)$$

3. Selection of the Candidate Core Size. Reference 5 defines the "relative power handling capacity" of the ATH core as

$$Q1 = 75 * \frac{W}{2} * A1 \quad (C-12)$$

Combining Eq. (C-12) with Eqs. (C-11) and (C-1),

$$Q1 = 1598 * Z * A2 \quad (C-13)$$

because

$$A2 = \frac{I1}{J} \quad (C-14)$$

therefore:

$$Q1 = 1598 * Z * \frac{I1}{J} \quad (C-15)$$

The candidate cores are listed in Table C-1. From this table, the computer selects a core Q2 that is slightly larger than Q1 size. This is the core used for the first design.

4. First Run for Q2-Size Core. With the core parameters fixed, the question arises whether all the constraints can be satisfied. Let us find out if Eq. (C-11) can be satisfied.

a. Number of 1/2 primary turns, N1. From Eq. (C-1),

$$N1 = \frac{Z}{A1} \quad (C-16)$$

As it is most likely that N1 contains a fraction, the computer rounds up the calculated number of turns to the integer portion, so that there is a little more winding space, and the flux density goes up slightly.

b. Wire cross section, A2. The maximum permissible current density in the conductor was specified under Subsection B-1 of this appendix. This means that A2 must be

$$A2 \geq \frac{I1}{J} \quad (C-17)$$

Scanning Table C-2 from the top to the bottom, a standard AWG size of wire is selected that is a shade smaller than the calculated A2 size. "Scanning" in this computer program means inserting the proper values of Q into Table C-2.

A recheck of the current density is performed. Using the A(Q, 2) cross section, the actual current density in the conductor must be less than the permissible maximum density J, thus:

$$\frac{I1}{A(Q, 2)} < J \quad (C-18)$$

in order to continue.

In the case where the Eq. (C-18) inequality has not been satisfied, the next larger Q2 core size is selected and all the above calculations are repeated. This iteration continues until the inequality of Eq. (C-18) is satisfied. The actual current density is then printed out and the design continues.

5. Iron Losses. The flux density is determined. From Eq. (C-3):

$$B = \frac{3.9 * V}{F1 * Z} \quad (C-19)$$

For the above value of B, the specific iron loss S1 is defined from Fig. A-6.

Iron loss per phase:

$$P1 = S1 * \frac{G1}{3} \quad (C-20)$$

where G1 is extracted from Table C-1.

6. Copper Losses. Total copper losses per phase are

$$P2 = 2I1^2 R1 + I2^2 R2 \quad (C-21)$$

In the case of a 1:1 transformation,

$$I2 = \sqrt{2} I1 \quad (C-22)$$

and for the same current density for both, the primary and the secondary winding resistances are

$$R2 = \frac{R1}{\sqrt{2}} \quad (C-23)$$

Consequently, combining Eqs. (C-21), (C-22), and (C-23),

$$P2 = 3.41 I1^2 R1$$

The above loss is increased by 30% to take care of such unspecified losses as eddy current losses, shield losses, and solder junction losses; thus,

$$P2 = 4.5 * I1^2 * R1 \quad (C-24)$$

where

$$R1 = N1 * S2 * \frac{L2}{12} * 10^{-3} \quad (C-25)$$

and (Fig. C-1)

$$L2 = 2 * (2E + D + F) \quad (C-26)$$

7. Total Transformer Loss. The inverter uses two three-phase transformers; thus, the total loss in iron and copper will be six times the value calculated above. A 20% safety margin is added to take care of unspecified losses such as air gap losses, and joint losses; thus,

$$P3 = 1.2 * 6 * (P1 + P2) \quad (C-27)$$

8. Transistor Losses. Transistor losses were computed by a separate calculation as shown in Appendix B and Figs. A-2, A-3, and A-4. The value of P6 is inputted into the computer as mentioned in Subsection B-1 of this Appendix.

9. Inverter Losses.

$$P4 = P3 + P6 \quad (C-28)$$

10. Inverter Efficiency.

$$E1 = 1 - \frac{P4}{(6 * P7)} \quad (C-29)$$

Adding losses in, for instance, the harness and connectors, the overall efficiency of the inverter is

$$E2 = 0.99 * E1 \quad (C-30)$$

Losses in the distribution bus are assumed to be 1.5%, thus:

$$E3 = 0.985 * E2 \quad (C-31)$$

11. Core Mass, 6 Phase. G1 is extracted from Table C-1 of core data. Two cores, in kg, will have a mass:

$$\frac{2G1}{2.2} \quad (C-32)$$

12. Copper Mass, 6 Phase. Mass of a single coil is determined by establishing the length of the wire of one coil, multiplying that length with the specific mass of the selected wire size. Six coils are used. Mass of the primary winding is

$$2 * N1 * L2 * S3 \quad (C-33)$$

Mass of the secondary winding is

$$N2 * L2 * \sqrt{2} * S3 \quad (C-34)$$

For six coils, the total mass is defined as:

$$G2 = 0.775 * 10^{-3} * N1 * L2 * S3 \quad (C-35)$$

13. Transformer Mass. An increase in the mass of iron by 20% is intended to cover the mass of the mounting hardware, epoxy (if needed), and others, thus:

$$G3 = \frac{2 * 1.2}{2.2} * G1 + G2 = 1.1 * G1 + G2 \quad (C-36)$$

14. Inverter Mass.

a. Without the radiator. The inverter mass consists of G3 plus the mass of transistors and mass of the mounting hardware. The estimated mass of one transistor complete with the mounting hardware is 0.150 kg. The 8-V system uses M = 24 transistors, and the higher voltage system uses M = 12 transistors per inverter. Mass of the logic circuits is estimated to be 0.7 kg; so,

$$G4 = G3 + 0.15 M + 0.7 \quad (C-37)$$

b. Mass of radiators. The specific mass of the inverter radiator, S7, varies for each case of environmental conditions. The values of S7 are listed in Table B-1. The mass of that radiator will be:

$$S7 * 6 * 10^{-3} * P7 * (1 - E2) \quad (C-38)$$

c. The inverter mass with radiator. This mass is defined from:

$$G5 = G4 + [S7 * 0.006 * P7 * (1 - E2)] \quad (C-39)$$

The total mass of all inverters is:

$$G6 = N * G5 \quad (C-40)$$

d. Mass of the power distribution, G7. The net mass of component parts, i. e., cables and isolation transformers, is estimated as 36.2 kg. Losses are estimated to be 600 W. The total mass with radiators is shown in Table C-3.

e. Mass of the power conditioners, G8. The net mass of components of a single power conditioner was estimated to be 10 kg. Losses per power conditioner, from Table 4, are 275.4 W. Using the specific mass of radiators as listed in Table B-1, the radiator and total power conditioner mass can be determined. Table C-4 lists the mass of all 27 power conditioners including the radiators.

f. Mass of the power processor, G9. The total mass of the power processor is derived as:

$$G9 = G6 + G7 + G8 \quad (C-41)$$

This is the mass plotted in Fig. 11.

15. Specific Mass.

a. Specific mass of the inverter and radiator.

$$S4 = 10^3 * G5/P5 \quad (C-42)$$

b. Specific mass inverter and radiator including the mass penalty in source.

$$S5 = S4 + P(1/E2 - 1) \quad (C-43)$$

It should be noted that P, the specific mass of the power source, has been defined for the 8-V system as 20 kg/kW, and for the 23- and 40-V systems as 15 kg/kW.

- c. Specific mass penalty in source.

$$S_6 = S_5 - S_4$$

- d. Specific mass of the complete power processor including radiators.

$$S_8 = S_4 + S_{\text{distr}} + S_{\text{PC}}$$

S8 is graphically shown in Fig. 11.

C. Printouts

Three categories of data are supplied by the program:

- (1) General data.
- (2) Design data, inverter.
- (3) Parametric data.

1. General Data. Printed are: input voltage, number of TFE sources, number of operating power conditioners, maximum power from TFEs, input power to 19 power conditioners, input power to 19 thrusters, and hotel loads.

2. Design Data, Inverter. The printout includes: frequency; core size (type); flux density; current density; wire size; number of primary turns; losses of copper, iron, transistor, miscellaneous, and total losses; electrical efficiency of the inverter; electrical efficiency of the inverter plus distribution.

3. Parametric Data. For each environmental case (1 through 8 of Table 1), data are printed of: inverter mass, single module and total; power processor total mass; the specific mass of the inverter; specific mass on penalty source; specific mass of inverter and source penalty; and, finally, the specific mass of the whole power processor.

D. Program

The program was written in XBASIC language. The program underwent a number of modifications, refinements, and improvements. It is preserved in the writer's file.

Table C-1. ATH core sizes and design parameters^a

D	E	F	G	K	G1	Q2	ATH
0.375	0.1875	0.5	1.125	0.85	0.25	6	43
0.75	0.125	0.4375	1	0.85	0.32	6.2	53
0.5	0.1875	0.625	1.625	0.85	0.44	14	25
0.625	0.1875	0.75	1.1875	0.85	0.59	15.6	55
0.75	0.25	0.5	1.125	0.85	0.75	15.8	83
0.75	0.25	0.625	1.5625	0.85	0.99	27	56
0.5	0.25	0.75	2	0.85	0.72	28	89
1	0.25	0.5	1.5625	0.85	1.15	29	78
0.75	0.25	0.6875	1.625	0.85	0.96	31	87
0.875	0.25	0.6875	1.625	0.85	1.06	37	66
1	0.25	0.6875	1.625	0.85	1.28	42	65
0.75	0.375	0.8125	1.25	0.85	1.53	43	31
1	0.25	0.75	2	0.85	1.45	56	90
1	0.375	0.6875	1.625	0.85	2.14	63	80
1.25	0.3125	0.625	1.9375	0.85	2.15	71	30
1.25	0.3125	0.6875	2.0625	0.85	2.26	83	58
1.25	0.3125	0.875	1.8125	0.85	2.36	93	61
1	0.375	1	1.75	0.85	2.47	99	95
1	0.375	1	2.375	0.85	2.8	133	85
1.25	0.4375	0.9375	1.875	0.85	3.78	144	70
1	0.375	1.25	2.5	0.85	3.05	176	35
1	0.375	1.25	2.5	0.85	3.8	220	4
1	0.5	1	3	0.85	4.51	225	92

^aSee Ref. 5 and Fig. A-5.

Table C-2. Wire data

Q	A(Q, 1)	A(Q, 2)	A(Q, 3)	A(Q, 4)
	Wire size, AWG	Cross section, in. ²	Resistance, Ω^a	Mass, lb ^a
1	3	0.04133	0.1971	159.3
2	4	0.03278	0.2485	126.3
3	5	0.02599	0.3134	100.2
4	6	0.02061	0.3952	79.44
5	7	0.01635	0.4981	63.03
6	8	0.01297	0.6281	49.98
7	9	0.01028	0.7925	39.62
8	10	0.00816	0.9988	31.43
9	11	0.00646	1.26	24.9

^aFor 1000-ft length.

Page intentionally left blank

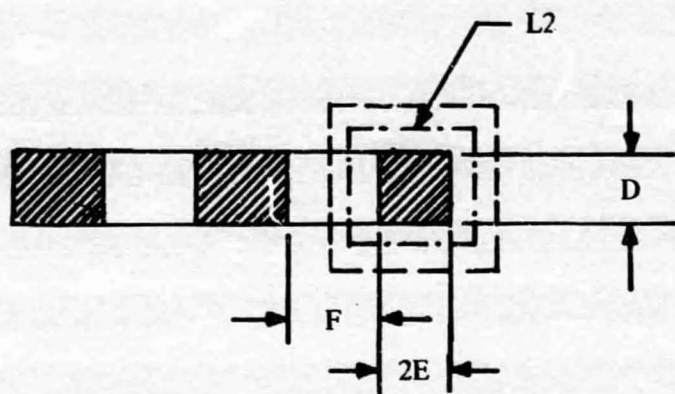


Fig. C-1. Three-phase E-core cross section and the middle length of a turn (L_2)

REFERENCES

1. Nuclear Electric Propulsion Mission Engineering Study Final Report, Vol. II, No. 73SD4219. General Electric Space Systems Organization, Valley Forge Space Center, Philadelphia, Penn., March 1973.
2. Macie, T. W., and Costogue, E. N., "Power Processing Requirements for Solar Electric Propulsion," presented at the IEEE-Power Conditioning Specialists Conference, Jet Propulsion Laboratory, Pasadena, Calif., April 19, 1971.
3. Masek, T. D., Solar Electric Propulsion Thrust Subsystem Development, Technical Report 32-1579. Jet Propulsion Laboratory, Pasadena, Calif., March 15, 1973.
4. Design and Development of a High Power, Low Saturation Voltage, Multichip Silicon Switching Transistor, Document No. 182724-1, Jet Propulsion Laboratory, Pasadena, Calif., February 1970 (internal document).
5. Power Conditioning and Control System for JPL 20-cm Electric Thruster, Vol. I, RFPC12-7420. 68(22)-3024/B6593-001. SSD80148P, Hughes Aircraft Co., El Segundo, Calif., April 1968.
6. Arnold Sillectron Cores, Bulletin SC-107A. Arnold Engineering Co., Marengo, Ill., 1963.
7. Ross, R., "Solar Electric Propulsion Power Conditioner Structural Design Study," IOM 358-72-116, Jet Propulsion Laboratory, Pasadena, Calif., Aug. 18, 1972 (internal document).
8. "Pioneer Disproves Asteroid Belt Hazards," *Aviat. Week*, Vol. 98, No. 9, pp. 66-69, Feb. 26, 1973.

SYMBOLS

A	computer address for Table C-2
ATH	core type, per Ref. 5
AWG	American wire gauge
A1	core cross section, in. ²
A2	copper wire cross section, in. ²
B	flux density, nominal, kG
D	core dimension (Fig. A-5 and Table C-1), in.
d	delay angle, deg
E	core dimension (Fig. A-5 and Table C-1), in.
$E_{CE \text{ sat}}$	saturation voltage, collector-emitter, V
E1	efficiency inverter without harness losses, per unit
E2	efficiency inverter with harness losses, per unit
E3	efficiency inverter with distribution, per unit
F	core dimension (Fig. A-5 and Table C-1), in.
F1	frequency, inverter, kHz
G	core dimension (Fig. A-5 and Table C-1), in.
G1	mass, core, 3-phase (Table C-1 or Ref. 5), lb
G2	mass, copper, 6 coils, kg
G3	mass, master and slave transformers, kg
G4	mass, inverter without radiator, kg
G5	mass, inverter with radiator, kg
G6	mass, all inverters, kg
G7	mass, power distribution, complete, kg
G8	mass, all power conditioners with the associated radiators, kg
G9	mass, power processor, complete, kg
Id	dc current, input, A

SYMBOLS (contd)

I_C	collector current, max, A
I_1	primary current, A
I_2	secondary current, A
J	current density, A/in. ²
K	stacking factor, $K = 0.85$ for 2-mil steel
L_2	mean length of a turn (Fig. C-1), in.
M	number of transistors per tandem inverter module, 6-phase inverter
N	number of inverters used, total
N_1	turns, 1/2-primary winding
N_2	turns, secondary winding
P	specific mass, source, kg/kW
p	penetration depth (Table A-1), mil
P_{sat}	saturation losses, W
P_{SW}	switching losses, W
P_1	iron loss transformer, 1-phase, W
P_2	copper loss transformer, 1-phase, W
P_3	total loss transformers, master and slave, W
P_4	Inverter loss, 6-phase, W
P_5	output power maximum, inverter, 6-phase, W
P_6	transistor losses, 6-phase inverter, W
P_7	input power, per phase, inverter, W
Q	line index for Table C-2
Q_C	copper cross section of one coil, in. ²
Q_{C1}	copper cross section, primary winding, in. ²
Q_{C2}	copper cross section, secondary winding, in. ²

SYMBOLS (contd)

Q1	required minimum size core, in. ⁴
Q2	core size available, from Table C-1, in. ⁴
R1	resistance N1 turns of wire, primary winding, Ω
R2	resistance N2 turns of wire, secondary winding, Ω
S _{distr}	specific mass, distribution, kg/kW
S _{PC}	specific mass, power conditioner, kg/kW
S1	specific iron loss, from Fig. A-6, W/lb
S2	specific resistivity, copper, from column 3, Table C-2, m Ω /ft
S3	specific mass, copper, from column 4, Table C-2, mlb/ft
S4	specific mass, inverter and radiator, kg/kW
S5	specific mass, inverter plus radiator and source penalty, kg/kW
S6	specific mass, penalty on source, kg/kW
S7	specific mass, radiator, kg/kW
S8	specific mass, power processor, kg/kW
T	period of the square wave
T _{SW}	switching time transistor, μ s
V	input dc voltage, V
W	window, total, in. ²
Z	design parameter, turns \times in. ²